CENTER FOR DRUG EVALUATION AND RESEARCH

APPLICATION NUMBER:

22-065

PHARMACOLOGY REVIEW

DEPARTMENT OF HEALTH AND HUMAN SERVICES
PUBLIC HEALTH SERVICE
FOOD AND DRUG ADMINISTRATION
CENTER FOR DRUG EVALUATION AND RESEARCH

PHARMACOLOGY/TOXICOLOGY REVIEW AND EVALUATION

NDA NUMBER:	**22, 065**
SERIAL NUMBER:	**000**
DATE RECEIVED BY CENTER:	**4/16/2007**
PRODUCT:	**Ixabepilone**
INTENDED CLINICAL POPULATION:	**breast cancer**
SPONSOR:	**Bristol Myers Squibb**
DOCUMENTS REVIEWED:	**Electronic Submission**
REVIEW DIVISION:	**Division of Drug Oncology Products**
PHARM/TOX REVIEWER:	**Robeena M. Aziz, MPH, PhD**
PHARM/TOX SUPERVISOR:	**John Leighton, PhD**
DIVISION DIRECTOR:	**Robert Justice, MD**
PROJECT MANAGER:	**Sharon Thomas**

Date of review submission to Division File System (DFS): **10/16/2007**

2.6 PHARMACOLOGY/TOXICOLOGY REVIEW

2.6.1 INTRODUCTION AND DRUG HISTORY

NDA number: 22, 065

Review number: 2 (Labeling Review)

Sequence number/date/type of submission: 000/April 16, 2007/Electronic NDA

Information to sponsor: Yes () No (X)

Sponsor and/or agent: Bristol-Myers Squibb Company
Wallingford, CT 06492

Manufacturer for drug substance: Bristol-Myers Squibb Company
Clinical supplies operation
Candiac, Quebec Canada

Reviewer name: Robeena M. Aziz, MPH, PhD

Division name: Division of Drug Oncology Products

HFD #: 150

Review completion date: October 11, 2007

Drug:

Trade name: IMEMPRA
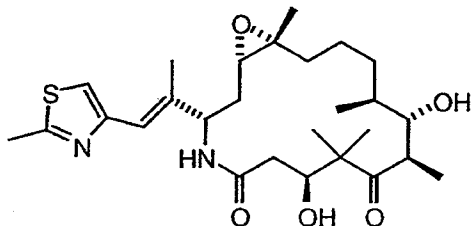Generic name: Ixabepilone

Code name: BMS-247550 or BMS-247550-01
Chemical name: [1S-[1R*, 3R*(E), 7R*, 10S*, 11R*, 12R*, 16S*]-7,11-Dihydroxy- 8,8,10,12,16- penta-methyl-3-[1-methyl-2-(2-methyl-4-thiazolyl)ethenyl]- 17-oxa-4-azabicyclo[14.1.0]heptadecane-5, 9-dione
CAS registry number:
Molecular formula/molecular weight: 506.7 / $C_{27}H_{42}N_2O_5S$
Structure:

Relevant INDs/NDAs/DMFs: 58, 546

Drug class: Microtubule inhibitor

Intended clinical population: breast cancer

Clinical Formulation: 15 and 45 mg/Vial for Injection.

| Component | Quality Standard | Label Potency | | Function |
| | | 15 mg/Vial | 45 mg/Vial | |
		Amount per Vial (mg)		
Ixabepilone	BMS[a] Specification	16.0[b]	47.0[c]	Active Ingredient

[a] Bristol-Myers Squibb

Route of administration: Intravenous infusion / solution

Indication:

- o In combination with capecitabine for the treatment of patients with metastatic or locally advanced breast cancer after failure of cytotoxic chemotherapy. Previous therapy should have included an anthracycline and a taxane.
- o As monotherapy for the treatment of metastatic or locally advanced breast cancer in patients whose tumors are resistant or refractory to cytotoxic chemotherapy. Previous therapy should include an anthracycline, a taxane, and capecitabine.

Starting dose: 40 mg/m^2 administered as a 3-hour infusion, once every 21 days.

**Appears This Way
On Original**

_7_ Page(s) Withheld

_____ Trade Secret / Confidential

_X_ Draft Labeling

_____ Deliberative Process

Memorandum

October 15, 2007

From: David Jacobson-Kram, Ph.D., DABT Office of New Drugs
To: Robert Justice, MD
Thru: John Leighton, Ph.D.

Subject: Review of pharmacology/toxicology section of NDA 22-065

I have reviewed the pharmacology/toxicology review of NDA ———— and the nonclinical toxicology/pharmacology section of the proposed drug label. I agree with the primary reviewer's conclusions and with the wording of the non clinical section of the package insert.

**Appears This Way
On Original**

MEMORANDUM

Date: October 11, 2007
From: John K. Leighton, PhD, DABT
Supervisory Pharmacologist
Division of Drug Oncology Products
To: File for NDA #22-065
Ixabepilone; Tradename to be determined
Re: Approvability for Pharmacology and Toxicology

Nonclinical studies that investigated the pharmacology and toxicology of ixabepilone provided to support the NDA for the treatment metastatic or locally advanced breast cancer were reviewed in detail by Dr. Robeena Aziz. The supporting nonclinical studies included information of the drug's pharmacology; pharmacokinetic and ADME; safety pharmacology; general toxicology (rat and dog); genetic toxicity (complete ICH battery); a fertility study in rats; and embryo-fetal developmental toxicity in rats and rabbits. The studies cited in the review by Dr. Aziz consist of original research conducted by the applicant.

The pharmacology studies submitted to the NDA suggest that cells may be sensitive to ixabepilone where they may be resistant to other microtubule inhibitors. Several hypothesis were given for this observation, but additional studies need to be conducted to more fully explore the mechanism of action of ixabepilone and translation to clinical utility. This is not an approval issue. In general toxicology studies, ixabepilone was toxic to rapidly dividing cells (GI, reproductive, and bone marrow) and to the peripheral nervous system. In genetic toxicity studies, ixabepilone was positive for clastogenicity in the *in vivo* rat micronucleus assay but was negative in other genotoxicity assays. Carcinogenic studies were not conducted for ixabepilone, nor are they needed for use in this patient population. Ixabepilone was negative for significant effects on fertility and teratogenesis. However, in the rat fertility study and the embryo-fetal developmental toxicity studies, numerous drug-related effects were observed. As Dr Aziz notes in her review, the pharmacokinetics in pregnant rabbits were not reliable and thus were dose-based; other comparisons are exposure-based. Pregnancy Category D is recommended based on embyro-fetal toxicity. These findings are consistent with other microtubule inhibitors, including the recommendation of the pregnancy category. The nonclinical findings are detailed in Dr. Aziz's Executive Summary and reflected in the product label.

A trade name for ixabepilone had not been finalized at the completion of Dr Aziz's review.

Recommendations: I concur with Dr. Aziz's conclusion that pharmacology and toxicology data support the approval of NDA 22-065, ixabepilone. There are no outstanding nonclinical issues related to the approval of ixabebilone.

DEPARTMENT OF HEALTH AND HUMAN SERVICES
PUBLIC HEALTH SERVICE
FOOD AND DRUG ADMINISTRATION
CENTER FOR DRUG EVALUATION AND RESEARCH

PHARMACOLOGY/TOXICOLOGY REVIEW AND EVALUATION

NDA NUMBER:	22, 065
SERIAL NUMBER:	000
DATE RECEIVED BY CENTER:	4/16/2007
PRODUCT:	Ixabepilone
INTENDED CLINICAL POPULATION:	breast cancer
SPONSOR:	Bristol Myers Squibb
DOCUMENTS REVIEWED:	Electronic Submission
REVIEW DIVISION:	Division of Oncology Drug Products (HFD-150)
PHARM/TOX REVIEWER:	Robeena M. Aziz, MPH, PhD
PHARM/TOX SUPERVISOR:	John Leighton, PhD
DIVISION DIRECTOR:	Robert Justice, MD
PROJECT MANAGER:	Sharon Thomas

Date of review submission to Division File System (DFS): **10/1/2007**

TABLE OF CONTENTS

EXECUTIVE SUMMARY

I.   Recommendations

A. Recommendation on approvability
Approvable. The non-clinical studies with intravenous infusion of ixabepilone support the safety of its use in metastatic breast cancer.

B. Recommendation for nonclinical studies
No additional non-clinical studies are required for ixabepilone

C. Recommendations on labeling
The recommendations to the sponsor's proposed labeling are given, with a detailed report regarding the rationale for the recommended changes, in a subsequent review.

II.   Summary of nonclinical findings

A. Brief overview of nonclinical findings
The nonclinical findings have shown the target sites of toxicity with ixabepilone to be gastrointestinal, hematopoietic (bone marrow and lymphoid tissue), and male reproductive system. In rats and dogs, peripheral neuropathy is also a target organ for toxicity. Many of these toxicities are seen in the clinic and are thought to be direct effects of the pharmacology of ixabepilone.

Ixabepilone was not mutagenic or clastogenic in the *in vitro* assays. Ixabepolone was clastogenic (induction of micronuclei) in the *in vivo* rat micronucleus assay at doses ≥ 0.625 mg/kg or 3.75 mg/m^2. These findings are commonly seen with microtubule-stabilizing agents.

Ixabepilone did not impair fertility when administered to either male or female rats prior to and during the mating time frame. It was not teratogenic in either the rat or the rabbit. It did, however, induce embryo-fetal toxicity in both species at doses that also caused maternal toxicity.

B. Pharmacologic activity
The pharmacological activity of ixabepilone is by stabilizing microtubule dynamics, resulting in blockade of cancer cells during the mitotic stage of the cell division cycle which leads to apoptosis and cell death. In nonclinical studies, ixabepilone showed low susceptibility to multiple tumor resistance mechanisms including efflux transporters, such as MRP-1 and P-glycoprotein (P-gp), which are involved in acquired and intrinsic drug resistance. The tubulin-binding mode of ixabepilone is effective in inhibiting the microtubule dynamics of multiple β-tubulin isoforms, including αβ-III tubulin compared to paclitaxel which inhibits αβ-II tubulin.

Ixabepilone showed activity in HCT116 (human colon cell line), MDR variant HCTVM46 cells, paclitaxel-resistant variant of A2780S (A2780Tax), and Pat-7 ovarian cell line expressing both MDR1 and MPR1. As monotherapy, ixabepilone has antitumor activity in 33 pf 35 human cancer xenografts. Prolonged tumor growth data equivalent to or greater than 1 log cell kill (LCK) was observed.

In vivo studies examining the combination of ixabepilone with several anticancer agents showed antitumor activity was significantly greater than observed as a single agent. Ixabepilone showed enhanced activity with capecitabine, cetuximab, bevacizumab, or trastuzumab. The drug showed modest activity enhancement when combined with irinotecan. The drug showed no enhancement when combined with gefitinib, gemcitabine or paclitaxel.

Ixabepilone is a microtubule inhibitor for pharmacological classification for labeling purposes. This is consistent with other drugs of this class that act by inhibiting microtubule function.

      C. Nonclinical safety issues relevant to clinical use

The nonclinical safety issues seen in the toxicology program with ixabepilone were toxicities to nerves and rapidly dividing cells, consistent with other microtubule inhibitors. In rodent toxicology studies, clinical signs of impaired limb function and righting reflex correlated with axonal/myelin degeneration in the sciatic nerve (6.7 mg/kg/week or 40.2 mg/m^2). Effects on sensory and motor nerve conduction were observed in rats (0.1 mg/kg/week or 0.6 mg/m^2) as part of safety pharmacology evaluation. In a non-rodent toxicology study, histopathological changes of minimal to mild axonal/myelin degeneration in nerves at injection sites were seen following treatment and the end of the recovery period (0.75 mg/kg/week or 15 mg/m^2).

In addition to the nervous system, the gastrointestinal system, hematolymphatic and reproductive systems are sites of toxicity in animal models. In the 6-month rat study, dosing with ixabepilone caused single cell necrosis and reactive hyperplasia of the glandular mucosa of the GI tract; atrophy of testes, epididymis, prostate gland, uterus and vaginal epithelium; and decreased thymus, testes, uterus, and prostate weights. The decreases in leukocyte (mainly lymphocytes and neutrophils) and reticulocytes counts correlated with bone marrow depletion and may have contributed to hematopoiesis in spleen. A dose-response was observed in these findings starting at 3 mg/kg/week (18 mg/m^2). In the 9-month dog study, toxicities included hematopoietic (bone marrow) and lymphoid depletion; gastrointestinal necrosis and reactive hyperplasia; and testicular degeneration. These findings occurred at 0.5 and 0.75 mg/kg/week (10 and 15 mg/m^2). In addition, decreases in testes, thymus, and epididymis weights, degeneration/atrophy of testes and necrosis and hyperplasia in epididymis were also observed at these doses. Dose-dependent decreases in the neutrophil count were observed in both rodents and non-rodents.

In vitro and *in vivo* cardiovascular safety pharmacology studies indicate that ixabepilone is unlikely to affect electrocardiographic parameters at anticipated plasma concentrations

in patients. In the hERG/IKr assay, ixabepilone inhibited currents by 13.5% at 30μM, indicating that ixabepilone showed a low potential for inhibition of K+ channels.

The highest percentages of radiolabeled-ixabepilone were detected in the liver, muscle, nonpigmented skin, and pigmented skin. Lower levels of were detected in the cerebellum, spinal cord, and testes, suggesting that the drug-derived radioactivity crossed the blood/brain and blood/testes barriers. In pregnant rats, ixabepilone-derived radioactivity was distributed in maternal and fetal tissues. Serum protein binding *in vitro* was higher in mouse compared to rats, dogs, and humans. Radiolabeled ixabepilione and metabolites were excreted into rat milk. The milk: plasma concentration ratios ranged from 0.296 to 2.64. The primary route of excretion of ixabepilone was fecal.

The profile of metabolites of ixabepilone is consistent across species, including rat, dog and human. These data were obtained from *in vitro* and *in vivo* studies in rats and dogs and *in vitro* studies from human hepatocytes. No metabolites were identified from human liver microsome preparations that were not also found in test species. In addition, metabolites were not cytotoxic in a colon carcinoma cell line, suggesting that metabolites do not contribute to ixabepilone overall toxicity.

The toxicities seen with ixabepilone are most likely an extension of the pharmacological action of the drug. In humans, ixabepilone toxicities were primarily manifested in the GI, hematopoietic, and peripheral nervous systems. Phase 1 clinical trials indicate that neutropenia, sensory neuropathy, myalgia and fatigue were the dose limiting toxicities. These effects were expected and consistent with the toxicity produced by other microtubule-stabilizing anticancer drugs.

In rat fertility studies, treated male rats were mated with treated female rats. Ixabepilone at 0.2 mg/kg (1.2 mg/m^2) induced paternal toxicity as evidenced by decreased body weights. In females (0.2 mg/kg/day or 1.2 mg/m^2) a decrease in body weight gain was noted. Embryo-toxicity was characterized by increased incidences of embryo lethality, decreases in litter size, and number of live fetuses. In embryo-fetal development study, pregnant rats were treated during the period of organogenesis [gestation day (GD) 6 to 15]. Ixabepilone at 0.3 mg/kg (1.8 mg/m^2), induced maternal toxicity (decreased body-weight gain and food consumption) and embryo-fetal toxicity (resorptions, decreased fetal bodyweights, and delayed fetal ossification). In pregnant rabbits treated during the period of organogenesis (GD7 to 19), ixabepilone at 0.3 mg/kg (3.6 mg/m^2) induced severe maternal toxicity resulting in mortality, and a marked increase in resorptions or abortions. The conclusion of these studies is that administration of ixabepilone during pregnancy may pose a risk for fetal toxicity. Pregnancy category D is recommended.

Mortality was observed in single dose rat and dog studies starting at 25 mg/kg or 150 mg/m^2 in rat and at 5 mg/kg or 100 mg/m^2 in dog. These findings are relevant for the potential for overdosing.

2.6 PHARMACOLOGY/TOXICOLOGY REVIEW

2.6.1 INTRODUCTION AND DRUG HISTORY

NDA number: 22, 065
Review number: 1
Sequence number/date/type of submission: 000/April 16, 2007/Electronic NDA
Information to sponsor: Yes () No (X)
Sponsor and/or agent: Bristol-Myers Squibb Company
                                 Wallingford, CT 06492

Manufacturer for drug substance: Bristol-Myers Squibb Company
                                 Clinical supplies operation
                                 Candiac, Quebec Canada
Reviewer name: Robeena M. Aziz, MPH, PhD
Division name: Division of Drug Oncology Products
HFD #:   150
Review completion date: September 21, 2007

Drug:
      Trade name:
      Generic name: Ixabepilone

      Code name: BMS-247550 or BMS-247550-01
      Chemical name: [1S-[1R*, 3R*(E), 7R*, 10S*, 11R*, 12R*, 16S*]]-7,11-Dihydroxy- 8,8,10,12,16- penta-methyl-3-[1-methyl-2-(2-methyl-4-thiazolyl)ethenyl]- 17-oxa-4-azabicyclo[14.1.0]heptadecane-5, 9-dione
      CAS registry number:
      Molecular formula/molecular weight: 506.7 / $C_{27}H_{42}N_2O_5S$
      Structure:

Relevant INDs/NDAs/DMFs: 58, 546

Drug class: Microtubule inhibitor

Intended clinical population: breast cancer

Clinical Formulation: 15 and 45 mg/Vial for Injection.

Component	Quality Standard	Label Potency		Function
		15 mg/Vial	45 mg/Vial	
		Amount per Vial (mg)		
Ixabepilone	BMS[a] Specification	16.0[b]	47.0[c]	Active Ingredient

[a] Bristol-Myers Squibb

Route of administration: Intravenous infusion / solution

Indication:

  o In combination with capecitabine for the treatment of patients with metastatic or locally advanced breast cancer after failure of cytotoxic chemotherapy. Previous therapy should have included an anthracycline and a taxane.

  o As monotherapy for the treatment of metastatic or locally advanced breast cancer in patients whose tumors are resistant or refractory to cytotoxic chemotherapy. Previous therapy should include an anthracycline, a taxane, and capecitabine.

Starting dose: 40 mg/m^2 administered as a 3-hour infusion, once every 21 days.

Disclaimer: Tabular and graphical information are constructed by the reviewer unless cited otherwise.

Appears This Way
On Original

Studies reviewed within this submission:

Pharmacology

Primary Pharmacodynamics:

	Title	Study No.	Module
1	Tubulin isotype expression of an inherently taxol-resistant, ixabepilone-sensitive human breast tumor	930014462	4.2.2.1
2	Binding of BMS-247550 to microtubules by isothermal titration calorimetry	930014465	4.2.2.1
3	Modulation by ixabepilone of microtubule dynamic instability of microtubules composed of different beta-tubulin isotypes	930014461	4.2.2.1
4	Further studies on the preclinical pharmacology of ixabepilone (BMS-247550), a novel microtubule stabilizer	930009639	4.2.2.1
5	Evaluation of ixabepilone (BMS-247550) degradants for *in vitro* cytotoxicity against a human tumor cell line panel	930014115	4.2.2.1

Secondary Pharmacodynamics:

	Title	Study No.	Module
1	Characterization of multidrug resistant cancer cell models	9600014464	4.2.2.1

Pharmacokinetic drug interactions:

	Title	Study No.	Module
1	Pharmacodynamic and PK studies to determine the minimum effective exposure of BMS-247550 required for anti-tumor activity *in vivo*	910074588	4.2.2.1

Safety Pharmacology:

	Title	Study No.	Module
1	The Comparison of the Effects of Ixabepilone and Taxol on Peripheral Nerve Function in the Rat: Electrophysiologic Measures	920014842	4.2.1.3
2	Effects of hERG Current and Rabbit Purkinje-Fiber Action Potentials	920009347	4.2.1.3

Pharmacokinetics

Repeat dose:

	Title	Study No.	Module
1	BMS-247550: Six month intermittent dose (Q21Dx10) intravenous toxicity study in rats II	DS03260/ 930011282	4.2.3.2
2	BMS-247550: Nine-Month Intermittent Dose (Q21x14) intravenous toxicity study in dogs	DS03196/ 930012300	4.2.3.2

Absorption:

	Title	Study No.	Module
1	Preliminary evaluation of the pharmacokinetics and metabolism of BMS-247550	MAP005/247550 /910074578	4.2.2.2

Distribution:

	Title	Study No.	Module
1	*In vitro* determination of serum protein binding and blood cell distribution of ixabepilone (BMS-247550) in mouse, rat, dog and human	930011862	4.2.2.3
2	Tissue Distribution and Excretion of Total Radioactivity Following Intravenous Administration of [^{14}C]BMS-247550 to Male and Female Long-Evans Rats – Tissue Distribution Report	6108-468(B)/ 930009762	4.2.2.3
3	Lacteal Excretion and Fetal Tissue Distribution of Radioactivity in Pregnant Female Sprague Dawley Rats and Tissue Distribution of Radioactivity in Male and Non-Pregnant Female Sprague Dawley Rats Following Intravenous Administration of [^{14}C]BMS-247550	6108-470/ 930010650	4.2.2.3

Appears This Way
On Original

Metabolism:

	Title	Study No.	Module
1	Comparative *in vitro* biotransformation of [^{14}C]ixabepilone (BMS-247550) in liver microsomal preparations of mice, rats, dogs, monkeys and humans	930009177	4.2.2.4
2	Evaluation of the *in vitro* cytotoxicity of a mixture of metabolites of ixabepilone (BMS-247550), which were generated in human liver microsomes, against a human colon carcinoma cell line	930019253	4.2.2.4

Excretion:

	Title	Study No.	Module
1	Tissue Distribution and Excretion of Total Radioactivity Following Intravenous Administration of [^{14}C]BMS-247550 to Male and Female Long-Evans Rats – Mass Balance Report	⎯⎯ 6108-468	4.2.2.5
2	Absorption, Metabolism, and Excretion of Total Radioactivity Following Intravenous Administration of [^{14}C]BMS-247550 to Dogs	⎯⎯ 6108-469	4.2.2.5
3	Biotransformation of [^{14}C] Ixabepilone ([^{14}C]BMS-247550) after Intravenous Administration to Bile Duct Cannulated (BDC) Rats	930012038	4.2.2.4
4	Metabolism of [^{14}C]Ixabepilone (BMS-247550) Following Intravenous Administration to Male and Female Rats and Dogs	930012773	4.2.2.4

Pharmacokinetic drug interaction:

	Title	Study No.	Module
1	*In Vitro* Evaluation of Ixabepilone (BMS-247550) as an Inducer of Cytochrome P450 Expression in Cultured Human Hepatocytes	XT043022/ 930012012	4.2.2.4
2	*In Vitro* Evaluation of Ixabepilone (BMS-247550) as an Inhibitor of Human Cytochrome P450 Enzymes	XT045016/ 930012272	4.2.2.4
3	A study to assess the potential for inhibition of human cytochrome P450 by BMS-247550	920007704	4.2.2.4
4	Identification of Enzymes Involved in the Metabolism of Ixabepilone (BMS-247550)	930012647	4.2.2.4
5	Investigation of the Enzymes Involved in the Oxidative Metabolism of Ixabepilone (BMS-247550), Study 2	930018090	4.2.2.4

Toxicology

Repeat Dose Studies:

	Title	Study No.	Module
1	BMS-247550: Six month intermittent dose (Q21Dx10) intravenous toxicity study in rats II	DS03260/ 930011282	4.2.3.2
2	BMS-247550: Nine-Month Intermittent Dose (Q21x14) intravenous toxicity study in dogs	DS03196/ 930012300	4.2.3.2

Genotoxicity:

	Title	Study No.	Module
1	BMS-247550: Ames Reverse-Mutation Study in Salmonella and *E. Coli*	DS01017/ 930000015	4.2.3.3
2	BMS-247550: Cytogenetics study in primary human lymphocytes	DS01012/ 930000096	4.2.3.3
3	BMS-247550: Intravenous micronucleus study in rats	DS03198/ 930006844	4.2.3.3

Reproductive and developmental toxicity:

	Title	Study No.	Module
1	Intravenous study of fertility and early embryonic development in rats	DN01028/ 930000931	4.2.3.5.1
2	BMS-247550: intravenous study of embryo-fetal development in rats	DN01009/ 930000517	4.2.3.5.2
3	Intravenous study of embryo-fetal development in rabbits	DN01014/ 930000804	4.2.3.5.2

_____1_____ Page(s) Withheld

_____✗_____ Trade Secret / Confidential

_____ Draft Labeling

_____ Deliberative Process

Other:

Studies previously reviewed within IND 58, 546:

Pharmacology

	Title	Study No.	Module
1	Preclinical pharmacology of BMS-247550, an epothilone analog	910074590	4.2.2.1

Pharmacokinetics

	Title	Study No.	. Module
1	BMS-247550 and paclitaxel: 5-day intravenous neurotoxicity study in mice	98915	-
2	Preliminary Evaluation of the PK and Metabolism of BMS-247550	MAP014/247550 /910074578	4.2.2.2

Toxicology
Single Dose Studies:

	Title	Study No.	Module
1	Single dose intravenous exploratory study in rats	98659	4.2.3.1
2	Single dose intravenous toxicity study in rats (GLP)	99612	4.2.3.1
3	Single dose intravenous toxicity study in dogs (GLP)	99617	4.2.3.1

2.6.2   PHARMACOLOGY

2.6.2.1 Brief summary

The epothilones and their analogs are a new class of non-taxane microtubule-stabilizing agents derived from the myxobacterium, *Sorangium cellulosum*, which has shown to have activity against taxane resistant cancer cell lines. Ixabepilone is a semi-synthetic analog of the natural epothilone B. Ixabepilone acts as an anti-neoplastic agent by stabilizing microtubule dynamics resulting in blockade of cancer cells in mitosis during cell division leading to cell death. Natural epothilones and their analogs have a tubulin-binding mechanism that is distinct from other microtubule-stabilizing agents. In non-clinical studies, ixabepilone has been shown to produce a low susceptibility to multiple tumor resistance mechanisms while retaining its activity in drug resistant cancer cell lines that overexpress drug efflux transporters such as MRP1 and P-glycoprotein (Pgp). Ixabepilone's tubulin-binding mode effects the microtubule dynamics of multiple β-II tubulin, including the taxane-resistant β-III isoform. *In vitro* and *in vivo* studies were conducted with ixabepilone to assess its mechanism of action.

Studies with Pat-21 (a human breast cancer model derived from a tumor sample in patients that are refractory to paclitaxel) indicate that it lacks a mutation in the tubulin sequence and does not express Pgp or MRP1. However, analysis of the β–tubulin isoform composition of this tumor reveals expression of βIII (1-13%) and absence of βII.

Studies examining the interaction of ixabepilone with tubulin by isothermal titration calorimetry (ITC) found that ixabepilone binds microtubules with an average apparent dissociation constant of 220 nM, suggesting direct binding of ixabepilone to microtubules.

In vitro studies examining the effects of ixabepilone and paclitaxel on the instability of microtubules showed that ixabepilone preferentially suppresses dynamic instability of αβ-III microtubules as compared with αβ-II microtubules. This is in contrast to paclitaxel which had no suppressive effect on the dynamic instability parameters of αβ-III microtubules while it suppressed parameters of αβ-II.

In vitro, ixabepilone demonstrated cytotoxic activity in three tissue specific tumor cell line panels including the breast (35 lines - IC_{50} values between 1.4 and 45 nM), colon (20 lines - IC_{50} values between 4.7 to 42 nM) and lung (23 lines- IC_{50} values between 2.3 to 19 nM). Ixabepilone had significant anti-tumor activity in 33 of 35 human cancer xenografts evaluated (consisting of 8 breast, 4 NSCLC, 4 pancreatic, 8 ovarian, 4 prostate, 4 colon, 1 SCLC, 1 gastric, and 1 squamous cell carcinoma with a prolonged tumor growth delay equivalent to or greater than 1 LCK in a majority of tumors. Ixabepilone was shown to overcome drug resistance due to the presence of the Pgp-mediated multi-drug resistance (MDR) phenotype thus reversing the established MDR resistance of MCF7/ADR and 16C/ADR breast carcinoma models *in vivo*. Combination studies with ixabepilone and other anticancer therapeutic agents showed anti-tumor activity was significantly greater than responses from the individual single agents administered at their MTD. Significant effects were observed with capecitabine, cetuximab, bevacizumab, or trastuzumab. Modest activity was observed when ixabepilone was combined with irinotecan. However, no difference in activity was observed when ixabepilone was combined with gefitinib, gemcitabine or paclitaxel.

Pharmacokinetic studies examining the minimum drug exposure required for ixabepilone to produce anti-tumor activity with human ovarian carcinoma cell lines *in vivo* showed the minimum effective concentration of ixabepilone in systemic circulation of mice required for anti-tumor activity compared to the Pat-7 human ovarian carcinoma cell line is 30-90 nM for a total infusion of 10 hours.

In vitro studies were conducted to determine if the degradants of ixabepilone has any effect on tumor cell growth. It was shown that the cytotoxic activity of all four degradants were substantially less active (39 to >312-fold) than ixabepilone when measured against a panel of breast, prostate, lung, colon, ovarian, and leukemia tumor cell lines.

In secondary pharmacodynamics studies, ixabepilone retained cytotoxic activity in human cancer cell lines that are resistant to common chemotherapeutic agents due to resistance mechanisms associated with expression of Pgp (MDR1), MRP1, or tubulin mutation. In the paclitaxel-sensitive human colon cell line HCT116, ixabepilone had an IC_{90} value of 7.3 nM compared to paclitaxel which had an IC_{90} of 18 nM (a 2.5-fold difference). In the MDR variant HCTVM46 cells (derived from the sensitive HCT116 parent cells), the difference in activity between paclitaxel and ixabepilone increased from 2.5 to 28.1-fold indicating a loss of activity of paclitaxel in HCTVM46 cells due to Pgp expression in these cells. Ixabepilone retained most of its activity in this highly MDR-expressing cell line. Similiar results were obtained for A2780Tax, a paclitaxel-resistant variant of A2780S, which is resistant to paclitaxel because of a tubulin gene mutation. In Pat-7 ovarian cell line expressing both MDR1 and MRP, paclitaxel had less cytotoxic activity with an IC_{90} value of 150 nM, whereas ixabepilone remained active with an IC_{90} value of 7.4 nM.

Ixabepilone was neurotoxic at a dose of 2 mg/kg in studies examining the peripheral nerve activity of ixabepilone compared to taxol in Wistar rats. This was evidenced by the presence of an altered nerve conduction. Peripheral neuropathy was still present at the 6-week recovery time point but there was some evidence of recovery at the low dose and for the tibial motor response in all groups. In the hERG assay, ixabepilone had no effect on any of the action potential parmeters measured in the Purkinje-fiber assay at 3, 10, and 30 µM.

2.6.2.2 Primary pharmacodynamics

910014462: Tubulin isotype expression of an inherently taxol-resistant, ixabepilone sensitive human breast tumor

Pat-21 is an early passage human breast cancer model derived from a tumor samples obtained from patients who are completely refractory to paclitaxel. The mechanism of resistance of this tumor model is not completely known. However, previous studies have shown this model does not to contain a mutation in its tubulin sequence nor does it express Pgp or MRP1. β-tubulin isoforms composition analysis of this tumor shows that it contains a small amount of βIII-tubulin (approximately 1-13%) and no βII-tubulin. The purpose of this study is to determine whether its β-tubulin composition can explain sensitivity to ixabepilone and resistance to taxanes in purified tubulin xenografted Pat-21 tumors. Xenografted Pat-21 tumors were excised from mice and the β-tubulin isotype content of Pat-21 tubulin was determined using quantitative gel electrophoresis and Western blotting. The results that are discussed below are from 4 repeats of electrophoresis and blotting for βI, βII, and βIV, five repeats for βIII, and one gel and blot for βV.

**Appears This Way
On Original**

13

The Figure below represents CoomassieBlue-stained SDS-PAGE gel of the electrophoresed tubulin samples. The doublet of bands represent α- and β-tubulin. High molecular weight microtubule-associated proteins (MAPs) are shown in lanes 3 and 4. The middle and lower panels indicate staining with anti- βIII-tubulin and anti-βV-tubulin, respectively. The arrow in lower panel shows anti-βV-stain in Pat21 and in HeLa tubulin (known to have ~80% βI-tubulin, no detectable βII-tubulin, no detectable βIII-tubulin, and 20% βIV-tubulin, Newton et al, *J. Biol. Chem.* 2002).

[Fig

**Appears This Way
On Original**

The figure below shows gels after staining with anti- βI-tubulin, anti-βII-tubulin, anti-βIII-tubulin and anti-βIV-tubulin.

Anti - ßI tubulin Anti-Body   Anti - ßII tubulin Anti-Body

Anti - ßIII tubulin Anti-Body   Anti - ßIV tubulin Anti-Body
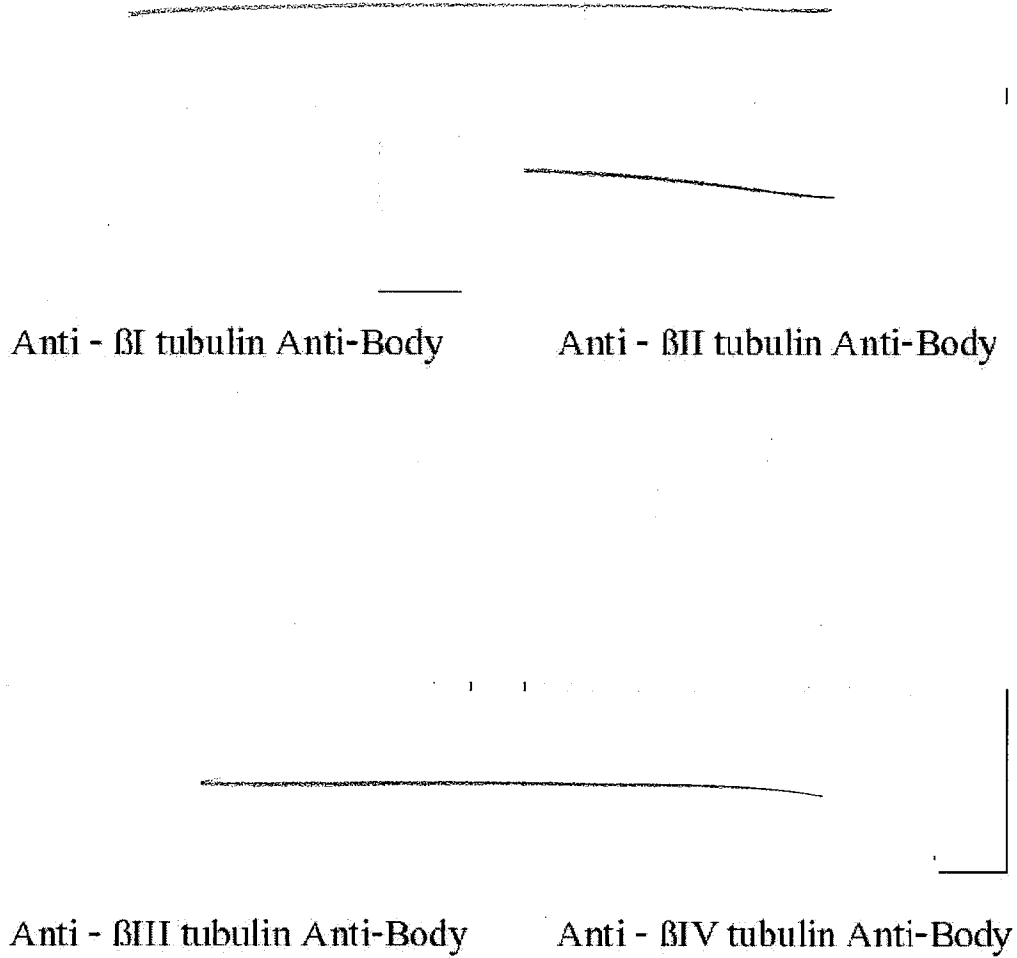
[Figure excerpted from Sponsor]

**Appears This Way
On Original**

The table shows quantitative immunoblotting of Pat-21 tubulin as compared with bovine brain tubulin and HeLa tubulin.

Table 1:   β-tubulin isotype distribution as percent of total β-tubulin

Isotype	Bovine Brain Tubulin[a]	HeLa Cell Tubulin[b]	Pat-21 Tumor Tubulin
βI - Tubulin	3	80	77
βII - Tubulin	58	0	0
βIII - Tubulin	25	0	1-13
βIV - Tubulin	13	20	11
βV - Tubulin	0	Trace	Trace

[a] from (Banerjee et al., 1988)

[b] from (Newton et al., 2002)

[Table excerpted from Sponsor]

Results of this study suggest that taxol resistance of Pat-21 may be due in part to changes in tubulin isotype composition, namely, a combination of loss of βII-tubulin expression of βIII-tubulin, and possible increases in expression of βV beta-tubulin. These levels are consistent with selective sensitivity to ixabepilone.

930014465:   Binding of BMS-247550 to microtubules by isothermal titration calorimetry.

This study examined the interaction of the epothilone B analog BMS-247550 (Ixabepilone) to tubulin by isothermal titration calorimetry (ITC). ITC has been used to study binding of microtubule destabilizers such as HTI-286 (a synthetic hemiasterlin analog), stathmin, and sulfonamides. No data showing the interaction of ITC with microtubule stabilizers such as taxanes and epothilones have been reported. BMS-247550 was found to bind preformed microtubules with an average apparent dissociation constant of 220 nM. Therefore, BMS-247550 has a direct binding to microtubules. Results from the three ITC experiments are summarized in the Sponsor's table below. The last line gives the average where it can be seen that the majority of the variability came from one titration.

**Appears This Way
On Original**

paclitaxel, ixabepilone is more effective at inhibiting proper formation of the mitotic spindle and successful completion of mitosis in tumor cells with significant expression of αβ-III tubulin. Data from this study are discussed and shown below.

Figure 1 shows representative traces of length changes at plus ends of individual microtubules over time. Microtubules are composed of purified αβ-II tubulin in (A, B) and are composed of purified αβ-III tubulin in (C, D). They are in the absence (A, C) or presence (B, D) of 25 nM ixabepilone. In controls (A, C), microtubules transitioned between periods of relatively slow growth and rapid shortening, and remained in a state of attenuated dynamic instability for significant periods of time. Transitions from slow growth or attenuation to rapid shortening are called "catastrophes", and transitions from shortening to growth or attenuation are called "rescues". In the presence of 25 nM ixabepilone (B, D), the rates of growth and shortening and the frequency of catastrophes were significantly reduced.

FIGURES AND LEGENDS

Figure 1 A-D. Growing and shortening at plus ends of individual microtubules composed of purified αβ-II (A, B), αβ-III (C,D) at steady state in the absence or presence of 25 nM ixabepilone. Shown are life-history traces of changes in length of individual untreated (control) microtubules (A,C) and individual microtubules in the presence of 25 nM ixabepilone (B, D). Tubulin concentrations: 12 μM αβ-II and 15 μM αβ-III-tubulin for controls. In the presence of ixabepilone, microtubules were longer and more numerous and it was necessary to reduce the tubulin concentrations to 7 μM αβ-II and 11 μM αβ-III-tubulin to facilitate measurement. Each trace (symbol) represents length changes of a single microtubule.

A- control αβ II;
B- αβ II with 25nM Ixabepilone

[Figure excerpted from Sponsor]

Figure 1 C and D

Time (minutes)
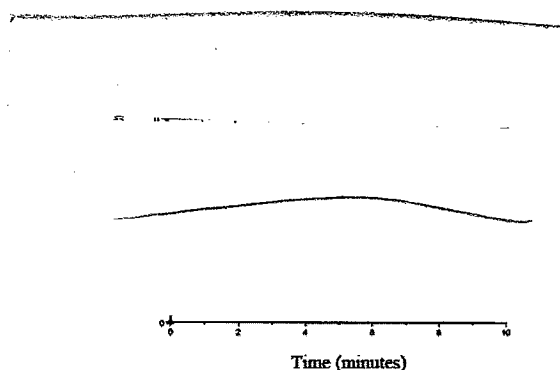
C- control $\alpha\beta$ III;
D- $\alpha\beta$ III with 25 nM Ixabepilone

[Figure excerpted from Sponsor]

930009639: Further studies on the preclinical pharmacology of ixabepilone (BMS-247550), a novel microtubule stabilizer.

The *in vitro* cytotoxicity of ixabepilone was evaluated in three tissue specific tumor cell line panels including the breast (35 lines), colon (20 lines) and lung (23 lines). In the 35 human breast cancer cell lines, ixabepilone demonstrated cytotoxicity with most IC_{50} values between 1.4 and 45 nM (a few cell lines exhibited resistance in the range >100 nM, See Sponsor's Figure 1A and 1B). In the 20 human colon tumor cell lines, ixabepilone showed cytotoxicity with most IC_{50} values ranging from 4.7 to 42 nM (2 lines with IC_{50} values that approached 100 nM or above, See Sponsor's Figure 2). All the 23 human lung carcinoma cell lines were sensitive to ixabepilone with IC_{50} values in the range of 2.3 to 19 nM (See Sponsor's Figure 3).

Appears This Way
On Original

Figure 1A: **Human Breast Cancer Cell line Panel A. Cytotoxicity Spectrum of Ixabepilone Versus a Panel of Human Breast Cancer Cell Lines.**

Bar graphs, on the right, depict the IC50 values of the cell lines listed on the left hand column (top to bottom).

BMS-247550		
Cell Line	IC50(uM)	± SD
AU-565	0.0024	0.0005
BT-20	0.0033	0.0014
BT-474	0.1434	0.0934
BT-549	0.0033	0.0017
H3396	0.0044	0.0007
HCC1419	0.0077	0.0028
HCC1428	0.0160	0.0116
HCC1806	0.0028	0.0011
HCC1954	0.0037	0.0009
HCC38	0.0030	0.0018
HCC70	0.0062	0.0033
HS578T	0.0075	0.0033
MCF7	0.0457	0.0393
MCF7/Her2	0.1559	0.0830
MDA-MB-157	0.0047	0.0024
MDA-MB-231	0.0056	0.0008
MDA-MB-435S	0.0035	0.0016
MDA-MB-436	0.0076	0.0016
MDA-MB-453	0.0047	0.0014
MDA-MB-468	0.0050	0.0011
SK-BR-3	0.0045	0.0016
ZR-75-1	>0.1974	0.0000
ZR-75-30	>0.1974	0.0000
Mean IC50	0.0098	
Median IC50	0.0050	
Min IC50	0.0024	
Max IC50	0.1974	
Range (Log Conc)	1.9226	

[Figure excerpted from Sponsor]

Appears This Way
On Original

Figure 2:   **Human Colon Cancer Cell line Panel. Cytotoxicity Spectrum of Ixabepilone Versus a Panel of Human Colon Cancer Cell Lines.**

Bar graphs, on the right, depict the IC50 values of the cell lines listed on the left hand column (top to bottom).

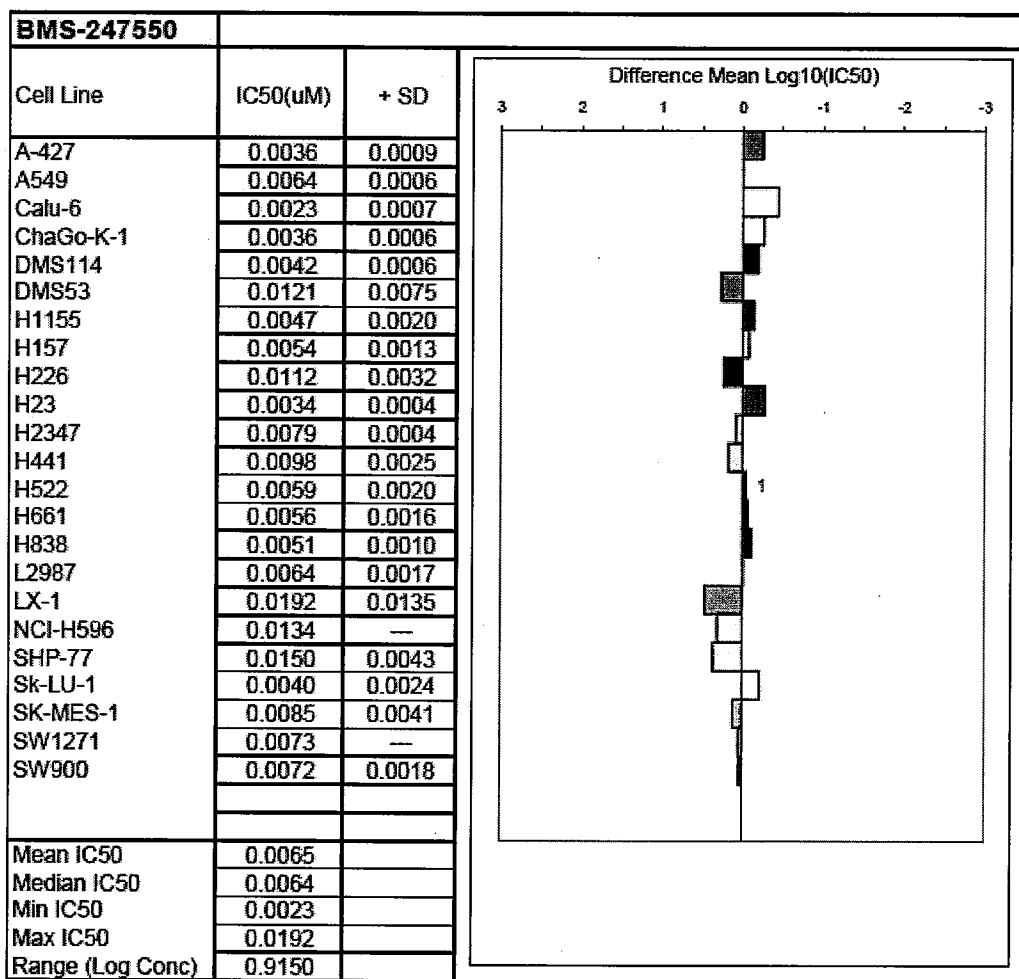| BMS-247550			Difference Mean Log10(IC50)
Cell Line	IC50(uM)	+ SD	
CCD-18Co	0.0497	0.0028	
CCD-33Co	0.0182	0.0063	
Colo201	0.0196	0.0124	
Colo205	0.0182	0.0090	
Colo320DM	0.0917	0.0332	
CX-1	0.0047	0.0012	
HCT-8	0.1974	0.0000	
LoVo	0.0155	0.0041	
SK-CO-1	0.0085	0.0035	
SW403	0.0089	0.0026	
SW1417	0.0050	0.0011	
SW480	0.0168	0.0052	
SW620	0.0086	0.0017	
SW837	0.0316	0.0172	
T84	0.0421	0.0284	
Caco-2	0.0406	0.0156	
HCT116	0.0094	0.0047	
HT-29	0.0095	0.0045	
LS174T	0.0313	0.0132	
MIP	0.0343	0.0162	
Mean IC50	0.0201		
Median IC50	0.0182		
Min IC50	0.0047		
Max IC50	0.1974		
Range (Log Conc)	1.6255		

[Figure excerpted from Sponsor]

Appears This Way
On Original

Figure 3:   **Human Lung Cancer Cell line Panel A. Cytotoxicity Spectrum of Ixabepilone Versus a Panel of Human Lung Cancer Cell Lines.**

Bar graphs, on the right, depict the IC_{50} values of the cell lines listed on the left hand column (top to bottom).

BMS-247550			
Cell Line	IC50(uM)	+ SD	Difference Mean Log10(IC50)
A-427	0.0036	0.0009	
A549	0.0064	0.0006	
Calu-6	0.0023	0.0007	
ChaGo-K-1	0.0036	0.0006	
DMS114	0.0042	0.0006	
DMS53	0.0121	0.0075	
H1155	0.0047	0.0020	
H157	0.0054	0.0013	
H226	0.0112	0.0032	
H23	0.0034	0.0004	
H2347	0.0079	0.0004	
H441	0.0098	0.0025	
H522	0.0059	0.0020	
H661	0.0056	0.0016	
H838	0.0051	0.0010	
L2987	0.0064	0.0017	
LX-1	0.0192	0.0135	
NCI-H596	0.0134	—	
SHP-77	0.0150	0.0043	
Sk-LU-1	0.0040	0.0024	
SK-MES-1	0.0085	0.0041	
SW1271	0.0073	—	
SW900	0.0072	0.0018	
Mean IC50	0.0065		
Median IC50	0.0064		
Min IC50	0.0023		
Max IC50	0.0192		
Range (Log Conc)	0.9150		

[Figure excerpted from Sponsor]

The anti-neoplastic activity of ixabepilone was also demonstrated against several human cancer xenografts in nude mice. Results from these studies showed ixabepilone had significant anti-tumor activity in 33 of 35 human cancer xenografts evaluated (consisting of 8 breast, 4 NSCLC, 4 pancreatic, 8 ovarian, 4 prostate, 4 colon, 1 SCLC, 1 gastric, and 1 squamous cell carcinoma – See Sponsor Table 1). In the majority of tumors, prolonged tumor growth delay equivalent to or greater than 1 LCK was achieved, which were accompanied by significant degree of tumor regression rates, both partial and complete.

Table 1　　　　　　Antitumor Efficacy of Ixabepilone as Monotherapy Against Human Tumor Xenografts

Tumor Type Tumor name	Dose [a,b]	Schedule	Antitumor Activity [a]			
			Growth Delay (Days)	LCK [c]	PR [c]	CR [c]	Cure

Tumor Type Tumor name	Dose [a,b]	Schedule	Growth Delay (Days)	LCK [c]	PR [c]	CR [c]	Cure
Breast							
BT474	6	Q7Dx3	≥ 128	> 3.4	75%	13%	0%
KPL-4	6	Q4D x 5	> 66.5	> 4.5	100%	100%	100%
MCF7	10	Q4D x 3	54	2.7	57%	0%	0%
MCF7/ADR	9	Q4D x 3	23.3	0.6	0%	0%	0%
MDA-MB-231	13	Q4D x 3	40	3.0	50%	38%	13%
MDA-MB-435	13	Q4D x 3	57.5	2.9	100%	13%	0%
Pat-14	9	Q4D x 3	> 76.5	> 1.6	100%	100%	0%
Pat-21	11.6	Q4D x 3	71.0	2.3	100%	29%	5%
Lung							
A549	11	Q4D x 3	47.5	1.3	17%	4%	0%
Calu-6	13	Q4D x 3	30.7	3.1	25%	0%	0%
L2987	10	Q4D x 3	66.2	4	100%	100%	75%
LX-1	10	Q4D x 3	> 67	> 7.5	100%	38%	0%
Pancreas							
Pat-24	10	Q4D x 3	> 45.8	> 1.8	71%	71%	29%
Pat-25	15	Q4D x 3	106	1.8	38%	25%	13%
Pat-26	10	Q4D x 3	23.5	1.2	20%	0%	0%
Pat-27	10	Q4D x 3	> 76	> 2.5	100%	71%	14%
Ovarian							
A2780s	16	Q4D x 3	≥ 47.5	> 5.3	100%	50%	50%
A2780Tax	6.3	Q2D x 5	23	2.5	0%	0%	0%
CD228	10	Q4D x 3	> 165.8	> 6.7	100%	100%	50%
MW387	10	Q4D x 3	37.5	0.8	75%	13%	13%
PA354	10	Q4D x 3	41.3	1.3	86%	29%	14%
Pat-7	10	Q4D x 3	25	2.4	88%	0%	0%
Pat-18	10	Q4D x 3	≥ 90.3	> 2.6	100%	75%	25%
Pat-22	10	Q4D x 3	> 156	> 3.6	100%	71%	57%
Prostate							
CWR-22	8	Q4D x 3	38.8	5.3	13%	0%	0%
LuCap35	8	Q4D x 3	> 28	> 1	75%	0%	0%
MDA-PCa-2b	12	Q4D x 3	58	2.2	25%	75%	-
PC3	12	Q4D x 3	69.5	4	50%	13%	13%
Colon							
GEO	10	Q4D x 3	15	1.1	0%	0%	0%
HCT-116	10	Q4D x 3	> 47.5	> 6.3	100%	63%	63%
HCT-116/VM46	16	Q4D x 3	26.8	2	0%	0%	0%
HT29	13	Q4D x 3	58.3	2.3	100%	86%	0%
SCLC							
NCI-H69	13	Q4D x 3	≥ 84.8	> 7.3	100%	88%	75%
Gastric							
N87	10	Q4D x 3	> 101.5	> 3.3	100%	63%	63%
Squamous							
A431	13	Q4D x 3	20.5	1.5	38%	13%	13%

[a] MTD; [b] All treatments were IV; [c] LCK= log cell kill; PR=partial regression; CR=complete regression

[d] Data from these studies are stored in the DDAPPS program. Unique identifiers for studies were generated within _____ a proprietary client-server DBMS running on a UNIX (Sun Solaris) server. Data is input and securely accessed from Windows machines running terminal emulation software. A listing of the Study Number for each tumor type is given in Appendix 2

[Table excerpted from Sponsor]

In a study to determine the relative antitumor activity of ixabepilone and docetaxel against Pat-21, a human breast cancer model (derived from a tumor biopsy obtained from a patient who was completely refractory to paclitaxel), ixabepilone showed significant activity producing antitumor effects of 1.6 LCK which was significantly greater than docetaxel which had a 0.2 LCK (P=0.003- See Sponsor's Figure 4 and Table 2).

Figure 4: Comparative Antitumor Efficacy of Ixabepilone and Docetaxel
          Against the Pat-21 Human Paclitaxel Resistant Breast Carcinoma

Results were from Study No. 1674. Each symbol represents the median
tumor burden of a group of 8 mice. (●) Control; (■) ixabepilone,
13 mg/kg/adm, Q4D x 3, IV; (△) docetaxel, 20 mg/kg/adm, Q2D x 5, IV.
For details of drug treatment see Materials and Methods.
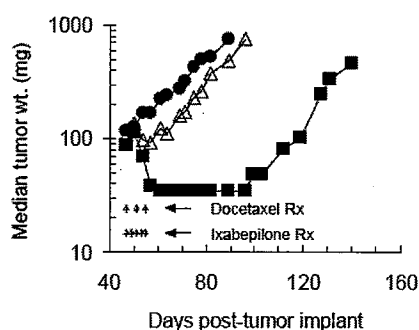
[Figure excerpted from Sponsor]

Table 2   **Comparison of the Antitumor Efficacy of Ixabepilone and Docetaxel
          in the Pat-21 Human Paclitaxel-Resistant Breast Carcinoma**

Study No.	Treatment Drug	Dose[a] (mg/kg)	Tumor Growth Delay[d] (LCK)	Wt. Change (days)	(g)	P
BMSR-1674	Ixabepilone	13[b]	1.6	67.5	-1.6	
	Docetaxel	20[c]	0.2	10.2	-1.4	0.003

[a] MTD; [b] Regimen: = IV, Q4D x 3; [c] Regimen: = IV, Q2D x 5; [d] Target tumor size = 500 mg

[Table excerpted from Sponsor]

The anti-tumor activity of ixabepilone and paclitaxel were determined against two Pgp-positive, multi-drug breast resistant models *in vivo*: MCF7/ADR and 16C/ADR. The 16C/ADR murine breast cancer model was derived from the parent 16C tumor line by repeat treatment of tumor-bearing mice with high dose adriamycin. The line shows resistance to ADR. Mice bearing 16C and resistant variant 16C/ADR tumors were treated with either adriamycin, paclitaxel or ixabepilone. Results showed that against the parent 16/C tumors, all three agents were highly active yielding anti-tumor activity of >3.7, 2.6 and >4.3 LCKs for adriamycin, paclitaxel and ixabepilone, respectively. Comparing with

the parent line, the 16C/ADR tumor was significantly less responsive to adriamycin (0.5 versus >3.7 LCK) and paclitaxel (1.4 versus 2.6 LCK) but remained highly sensitive to ixabepilone (3.5 versus >3.7 LCK). At their respective MTD, ixabepilone was significantly more active than paclitaxel in the 16C/ADR model (P=0.0048). In the second MDR model, MCF7/ADR, ixabepilone produced 0.5 LCK, compared to 0 LCK for paclitaxel, the difference between the two treatments was statistically significant (P=0.04). Results are summarized in the Sponsor's table below.

Table 3   **Comparison of the Antitumor Efficacy of Adriamycin, Ixabepilone and Paclitaxel Against the 16/C Mammary Carcinoma and the Multidrug Resistant (MDR) Variant 16C/ADR**

Drug (dose) [a]	Tumor	Efficacy	
		Tumor Growth Delay [d]	
		(LCK)	(days)
Adriamycin (6 mg/kg) [b]	16C	>3.7	>24.7
	16C/ADR	0.5	3.3
Paclitaxel (36 mg/kg) [c]	16C	2.6	27.5
	16C/ADR	1.4	9
Ixabepilone (10 mg/kg) [b]	16C	>3.7	>28.7
	16C/ADR	3.5	23.5

[a] MTD; [b] Regimen: = IV, Q4D x 3; [c] Regimen: = IV, Q2D x 5; [d] Target tumor size = 500 mg

Table 4   **Comparison of the Antitumor Efficacy of Ixabepilone and Paclitaxel Against Two Pgp-positive Multidrug Resistant (MDR) Breast Carcinomas**

Tumor/ Study No.	Treatment		Efficacy		
	Drug	Dose [a]	Tumor Growth Delay [d]		
		(mg/kg)	(LCK)	(days)	P
16C/ADR No. 4	Ixabepilone	10 [b]	3.5	23.5	
	Paclitaxel	36 [c]	1.4	9	0.0048
MCF7/ADR BMSR-1116	Ixabepilone	6.3 [c]	0.5	16.5	
	Paclitaxel	36 [c]	0	0.8	0.04

[a] MTD; [b] Regimen: = IV, Q4D x 3; [c] Regimen: = IV, Q2D x 5

[d] Target tumor size = 500 mg for MCF/ADR and 1000 mg for 16C/ADR

[Tables excerpted from Sponsor]

The combination of ixabepilone with a several anticancer agents was evaluated to determine if the anti-tumor activities are greater than the MTD of individual agents. Significant effects were observed with capecitabine, cetuximab, bevacizumab, or trastuzumab. Modest activity was observed when ixabepilone was combined with irinotecan. However, no difference in activity was observed when ixabepilone was combined with gefitinib, gemcitabine or paclitaxel. See Sponsor's Tables below.

Table 5   Antitumor efficacy of Combined Chemotherapy with Ixabepilone and Capecitabine Versus the GEO Human Colon Carcinoma

	Treatment		Efficacy/Toxicity			
	Ixabepilone	Capecitabine	Tumor		Wt.	
	Dose [a,b]	Dose [a,c]	Growth Delay [d]		Change	
Study No.	(mg/kg)	(mg/kg)	(LCK)	(days)	(g)	P
BMSR-1569	10	–	0.8	11	-3.8	0.035
	-	250	0.4	5.5	0.2	0.0004
	10	250	1.9	25.2	-4.9	-
BMSR-1767	10	–	1.2	18.7	-4.2	0.0037
	-	250	0.6	9.7	-0.3	0.0038
	10	250	3.9	62	-4.2	-

[a] MTD; [b] Regimen: = IV, Q4D x 3; [c] Regimen: = PO, QD x 10; [d] Target tumor size = 1000 mg

Table 6   Synergistic Antitumor Efficacy of Combined Chemotherapy with Ixabepilone and Cetuximab in the Human Colon Carcinoma GEO and Lung Carcinoma L2987

	Treatment		Efficacy			Toxicity	
	Ixabepilone	Cetuximab	Tumor			Wt.	
Tumor/	Dose [a,b]	Dose [c,d]	Growth Delay [e]		Cures	Change	
Study No.	(mg/kg)	(mg/kg)	(LCK)	(days)	(%)	(g)	P
GEO	10	-	1.1			-3.9	0.0173
BMSR-1709	-	0.25	0.8			0.4	0.0002
	10	0.25	1.7			-3.9	-
L2987	6	-	3.2	52.3	13	-4.7	0.011
No. 140	-	1	3	49.7	13	1.8	0.023
	6	1	>3.8	>63.2	75	-4.8	-
L2987	6	-	3.1	40.7	0	-4.4	0.0057
No. 143	-	1	2.4	32.2	0	1.4	0.0017
	6	1	>6.5	>86.7	38	-4.2	-

[a] MTD; [b] Regimen: BMSR-1709 = IV, Q4D x 3; L2987-140 and L2987-143 = IV, Q4D x 5; [c] OD,

[d] Regimen: BMSR-1709 = IP, Q3D x 4; L2987-140 and L2987-143 = IP, Q3D x 6;

[e] Target tumor size = 500 mg

Table 7   Synergistic Antitumor Efficacy of Combined Chemotherapy with Ixabepilone and Bevacizumab in the L2987 Human Lung Carcinoma

	Treatment		Efficacy					Toxicity	
	Ixabepilone	Bevacizumab	Tumor		Regression			Wt.	
Tumor/	Dose [a,b]	Dose [c,d]	Growth Delay [e]		PR	CR	Cures	Change	
Study No.	(mg/kg)	(mg/mouse)	(LCK)	(days)	(%)	(%)	(%)	(g)	P
L2987	6	-	3	29.8	38	0	0	-4	0.0031
L2987-145	-	4	2	19.8	0	0	0	0.7	0.0008
	6	4	>5.9	>59	33	50	50	-3.4	-

[a] MTD; [b] Regimen: IV, Q4D x 4; [c] OD; [d] Regimen: IP, Q4D x 4; [e] Target tumor size = 500 mg

Appears This Way
On Original

Table 8   Synergistic Antitumor Efficacy by Combined Chemotherapy with Ixabepilone and Trastuzumab Versus KPL4 Human Breast Carcinoma

Study No.	Ixabepilone Dose [a,b] (mg/kg)	Trastuzumab Dose [c,d] (mg/kg)	LCK	Growth Delay [e] (days)	% Cure	Wt. Loss (g)	P
KPL4	4	–	0.9	17	0	-1.5	0.0061
BMSR-1951	-	10	0	0	0	0.1	0.0034
	4	10	> 3.7	> 74	50	-3	–

[a] MTD; [b] Regimen: = IV, Q4D x 5; [c] OD or highest test dose; [d] Regimen: = IP, Q4D x 5;

[e] Target tumor size = 500 mg

Table 11   Antitumor Efficacy of Combined Chemotherapy with Ixabepilone and CPT-11 Versus the Human Colon Carcinoma GEO

Tumor Study No.	Ixabepilone Dose [a,b] (mg/kg)	CPT-11 Dose [a,c] (mg/kg)	Tumor Growth Delay [d] (LCK)	(days)	P
GEO					
BMSR-1569	10	–	1.4	21.2	0.0004
	-	36	1.7	25.7	0.0272
	10	36	2.2	32.7	–

[a] MTD; [b] Regimen: = IV, Q4D x 3; [c] Regimen: = IV, Q2D x 5; [d] Target tumor size = 1000 mg

Table 9   Antitumor Efficacy by Combined Chemotherapy with Ixabepilone and Gefitinib Versus the EGFR Positive A549 Human Lung Carcinoma

A549 Study No.	Ixabepilone Dose [a,b] (mg/kg)	Gefitinib Dose [c,d] (mg/kg)	Tumor Growth Delay [e] (LCK)	(days)	Wt. Change (g)	P
A549-49	10	–	1.7	31.5	-2.8	0.4899
	-	200	0.6	12	-0.7	0.0049
	10	100	1.5	28	-4.1	–

[a] MTD; [b] Regimen: = IV, Q4D x 3; [c] MTD; [d] Regimen: = PO, QD x 14; [e] Target tumor size = 500 mg

Table 10   Antitumor Efficacy of Combined Chemotherapy with Ixabepilone and Paclitaxel Versus the Human Pancreatic Carcinoma Pat-26

Pat-26 Study No.	Ixabepilone Dose (mg/kg)	Paclitaxel Dose (mg/kg)	Combination Schedule	Tumor Growth Delay [c] (LCK)	(days)	P
BMSR-1138	13	–		0.7	24.3	1
	-	30		0.1	2	0.0002
	9	18	Ixabepilone 3 hr before Ptxl	0.6	20.5	0.5955
	9	18	Ixabepilone 2 days before Ptxl	0.8	30.8	0.5223

[a] MTD; [b] Regimen: = IV, Q4D x 3; [c] Target tumor size = 500 mg

Table 12   **Antitumor Efficacy of Combined Chemotherapy with Ixabepilone and Gemcitabine Versus the Human Pancreatic Carcinoma Pat-26**

Pat-26	Treatment		Efficacy		
	Ixabepilone	Gemcitabine	Tumor		
	Dose [a, b]	Dose [a,c]	Growth Delay[d]		
	(mg/kg)	(mg/kg)	(LCK)	(days)	P
BMSR-1881	6	–	2.2	52.3	0.3968
	–	36	0.5	12	0.0017
	6	18	2.6	63	–

[a] MTD;   [b] Regimen = IV, Q4D x 5;   [c] Regimen = IV, Q4D x 5;   [d] Target tumor size = 500 mg
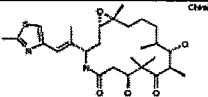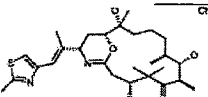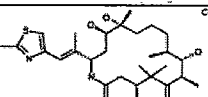
[Tables excerpted from Sponsor]

910014115:   Evaluation of Ixabepilone (BMS-247550) degradants for *in vitro* cytotoxicity against a human tumor cell line panel.

Degradants of ixabepilone ——————— BMS-249798, BMS-326412, ———— ———) were examined for its *in vitro* cytotoxicity against a panel of 12 human tumor cell lines. The human tumor cell line panel that was evaluated included: breast carcinoma cell lines (BT-549, DU4475, MDA-MB-468, MDA-MB-231); prostate carcinoma cell lines (LNCAP-FGC, PC-3, DU145); lung carcinoma (NCI-H446, SHP-77); colon carcinoma cell line (HCT116); ovarian carcinoma cell line (A2780/DDP-S); and leukemia cell line (CCRF-CEM). *In vitro* cytotoxicity was assessed using MTS assay. IC_{50} values were determined after 72 hour drug exposure for each of the cell lines against the degradants, plus BMS-247550 which was run as a standard. Mean IC_{50} values were calculated from all the individual cell line IC_{50} values for each compound. Based on previous studies, BMS-247550 has a mean IC_{50} value of 0.0066 µM.

Results of this study are shown in the table and figure below. All the degradants were significantly less active than BMS-247550. ——————————————————— had a mean IC_{50} value of 0.241 µM (a 39-fold loss in activity). For the other three degradants (BMS-249798, BMS-326412, _____) the loss in activity was substantially greater, 174 to >312-fold. The loss of activity may be attributed to the fact that the ____ ————————————————————————————————— The epoxide ring is a key structural component in the ixabepilone molecule which is necessary for its activity on tubulin polymerization.
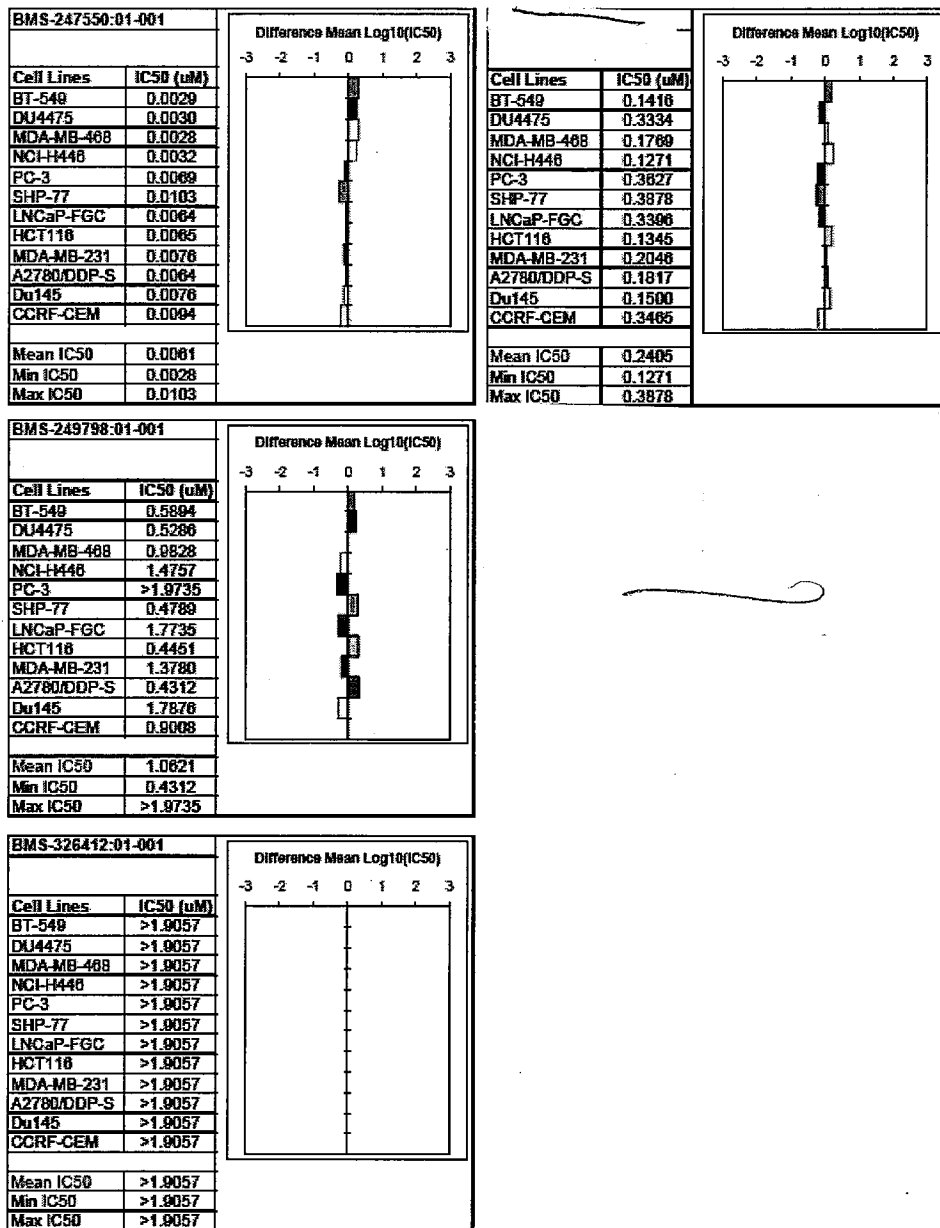
**Appears This Way
On Original**

Table I. In Vitro Cytotoxicity of Degradants of BMS-247550

Compound	Structure	Cell Panel Mean IC50 (uM)	Fold Loss in Potency*
BMS-247550		0.0061	1
		0.2405	39
BMS-249798 Epoxide opened, new 6-membered ring rearrangement		1.0621	174
		>1.9057	>312
BMS-326412 Epoxide opened by water addition rearrangement		>1.9057	>312

*Relative to BMS-247550

[Table excerpted from Sponsor]

Appears This Way
On Original

Figure 1:   In Vitro Cytotoxicity of BMS-247550 and degradants evaluated against a human tumor cell line panel after 72 hour drug exposure.

BMS-247550:01-001

Cell Lines	IC50 (uM)
BT-549	0.0029
DU4475	0.0030
MDA-MB-468	0.0028
NCI-H446	0.0032
PC-3	0.0069
SHP-77	0.0103
LNCaP-FGC	0.0064
HCT116	0.0065
MDA-MB-231	0.0076
A2780/DDP-S	0.0064
Du145	0.0076
CCRF-CEM	0.0094
Mean IC50	0.0061
Min IC50	0.0028
Max IC50	0.0103

BMS-247550 (second panel)

Cell Lines	IC50 (uM)
BT-549	0.1416
DU4475	0.3334
MDA-MB-468	0.1769
NCI-H446	0.1271
PC-3	0.3627
SHP-77	0.3878
LNCaP-FGC	0.3396
HCT116	0.1345
MDA-MB-231	0.2046
A2780/DDP-S	0.1817
Du145	0.1500
CCRF-CEM	0.3465
Mean IC50	0.2405
Min IC50	0.1271
Max IC50	0.3878

BMS-249798:01-001

Cell Lines	IC50 (uM)
BT-549	0.5894
DU4475	0.5286
MDA-MB-468	0.9828
NCI-H446	1.4757
PC-3	>1.9735
SHP-77	0.4789
LNCaP-FGC	1.7735
HCT116	0.4451
MDA-MB-231	1.3780
A2780/DDP-S	0.4312
Du145	1.7876
CCRF-CEM	0.9008
Mean IC50	1.0621
Min IC50	0.4312
Max IC50	>1.9735

BMS-326412:01-001

Cell Lines	IC50 (uM)
BT-549	>1.9057
DU4475	>1.9057
MDA-MB-468	>1.9057
NCI-H446	>1.9057
PC-3	>1.9057
SHP-77	>1.9057
LNCaP-FGC	>1.9057
HCT116	>1.9057
MDA-MB-231	>1.9057
A2780/DDP-S	>1.9057
Du145	>1.9057
CCRF-CEM	>1.9057
Mean IC50	>1.9057
Min IC50	>1.9057
Max IC50	>1.9057

[Figure excerpted from Sponsor]

Appears This Way
On Original

1.6.2.3 Secondary pharmacodynamics

930014464: Characterization of multi-drug resistant cancer cell models

Three paclitaxel-resistant human cancer models were characterized for the existence of various resistance mechanisms. The cell lines that were studied were the multidrug resistant human colon carcinoma cell line (HCTVM46), the human ovarian carcinoma cell line (Pat-7) and the human breast carcinoma cell lines (Pat-21). Results showed that HCTVM46 has a high overexpression of the multidrug resistance efflux pump (170 Kd P-glycoprotein, Pgp) as shown by flow cytometry and Western blot analysis. Further assays showed that HCTVM46 demonstrated efficient efflux of the Pgp substrates Rh123 and paclitaxel. However, HCTVM46 was not efficient in effluxing ixabepilone thus causing accumulation of ixabepilone inside HCTVM46 cells. In addition, HCTVM46 did not have any effect on MRP1 expression and no tubulin mutation was detected. In contrast, Pat-7 exhibited an overexpression of MRP1 as well as a significant expression of Pgp. However no tubulin mutation was detected in this line. Pat-21 had undetectable expression of Pgp or MRP1 and had no detectable tubulin mutation. The Sponsor concluded that the mode of paclitaxel resistance of Pat-21 must be related to other mechanisms.

A. *In vitro* characterization of multidrug resistant cell line HCTVM46

1. **Differential cytotoxicity of ixabepilone and paclitaxel in the paclitaxel resistant HCTVM46 Pgp overexpressing colon carcinoma cell line**
   The Sponsor's Table below shows the parent HCT116 human colon carcinoma cell line and its Pgp overexpressing variant HCTVM46 being tested for sensitivity to paclitaxel and ixabepilone using a colony formation assay. As shown, Pgp (MDR1) overexpressing HCTVM46 was 25-fold more resistant to paclitaxel than its parent line HCT116. By contrast, HCTVM46 was only 2.2-fold more resistant to ixabepilone than the parental HCT116.

Table 1		Clonogenic cytotoxicity of paclitaxel and ixabepilone in HCT116 and HCTVM46 human colon carcinoma cell lines		
		Cytotoxicity IC_{90}[a] (nM)		
Compound	Expt. No.	HCT116	HCTVM46	Ratio[b]
Paclitaxel	410, 168	18.0	450	25.0
Ixabepilone	369	7.3	16	2.2

[a] IC_{90} is defined as the concentration of the agent to affect a 90% reduction of survival of the clonogenic cancer cell population

[b] the ratio of IC90 values for HCTVM46/HCT116

[Table excerpted from Sponsor]

2. HCTVM46 overexpresses Pgp as determined by flow cytometry and Western blot analysis

The Figure B below shows that paclitaxel-resistant HCTVM46 expressed a high level of the *MDR1* encoded Pgp protein as detected by FAC analysis of cells using the 4E3 monoclonal antibody. In comparison, the parent paclitaxel-sensitive HCT116 cell line demonstrated absence of Pgp expression (Figure A).
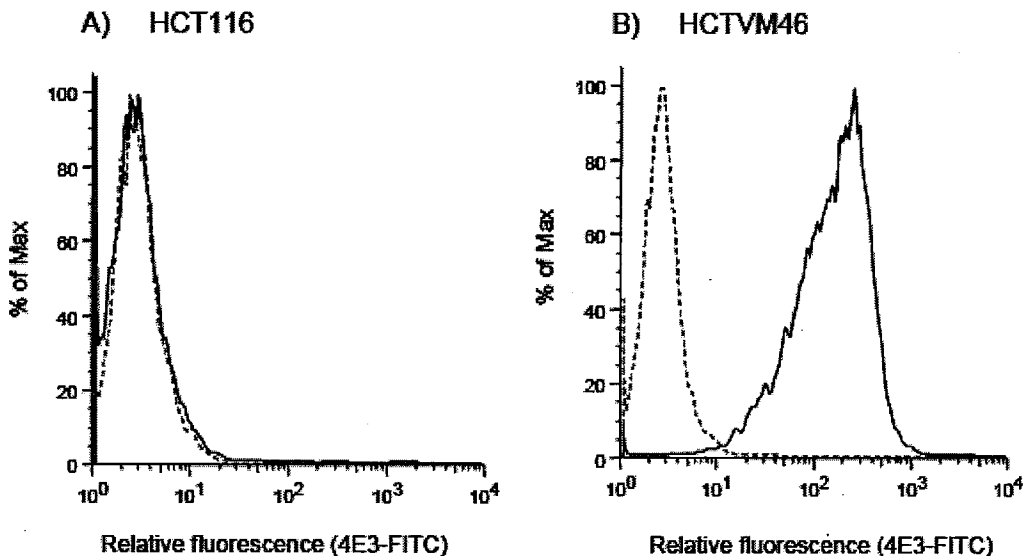

Figure 1. Comparative Pgp expression in the parent HCT116 (A) and the Pgp overexpressing HCTVM46 (B) human colon carcinoma cell lines.

The Figure below depicts results of Western blot analyses of Pgp and MRP1 expression in various human cancer cell lines. The multidrug resistant HCTVM46 overexpressed Pgp in contrast to the parent paclitaxel-sensitive HCT116 which did not. Of al the 8 cell lines analyzed, only Pat-7 expressed Pgp.
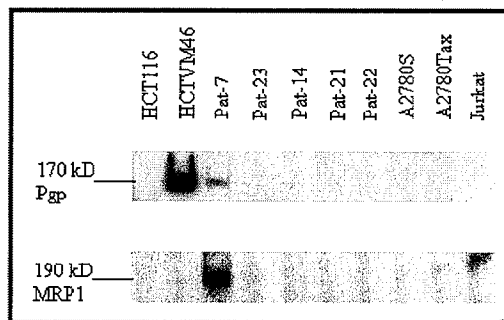
Western blot analysis of Pgp and MRP1 expression in various human cancer cell lines: HCT116 and HCTVM46 (colon carcinoma), Pat-7, A2780S, A2780Tax, Pat-22 and Pat-23 (ovarian carcinoma), Pat-14 and Pat-21 (breast carcinoma), and Jurkat (T cells).

[Figures excerpted from Sponsor]

3. **Functional assay of Pgp activity in HCTVM46 as determined by Rh123 retention**

The Figure below shows results of the assay that measured the accumulation and efflux of Rh123 in the HCT116 human colon carcinoma cell line and its Pgp overexpressing MDR variant HCTVM46. Rhodamine 123 (Rh123) is a fluorescent dye which accumulates in the mitochondria of cells. It is a substrate for Pgp and can, therefore, be used as a molecular probe in studies of the multidrug resistance (MDR) phenotype. In HCT116 cells, Rh123 accumulates rapidly in a concentration dependent manner up to ~62.5 ng/mL following a 30 min incubation. In HCTVM46 cell (which overexpresses Pgp and is 25-fold resistant to paclitaxel clonogenic cytotoxicity) accumulation is dramatically reduced. The data suggest that the Pgp protein expressed in HCTVM46 functional and was responsible for the efflux of Rh123 from these cells.
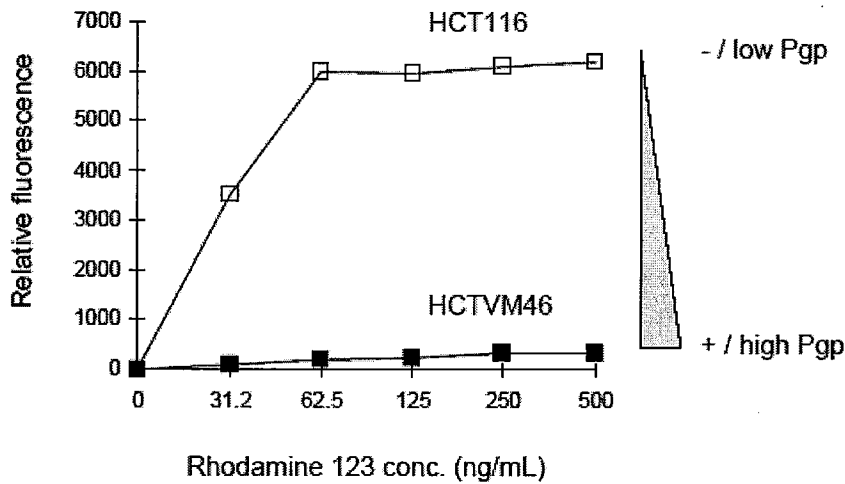
Figure 3. **Comparative rhodamine 123 (Rh123) retentions in the parent HCT116 and the Pgp overexpressing HCTVM46 human colon carcinoma cell lines.**

HCT116 (□) and the Pgp overexpressing HCTVM46 (■) human colon carcinoma cell lines. Results were from Study No. BMSR-132

[Figure excerpted from Sponsor]

Appears This Way
On Original

4. Differential cellular uptake of paclitaxel and ixabepilone into HCTVM46 cells

Paclitaxel and ixabepilone were incubated with the parent HCT116 cells (non-Pgp expressing) and the MDR variant HCTVM46 cells at the therapeutic concentration of 20 nM. Intracellular drug concentrations were assayed at intervals from 0 to 2.0 hr. Results from this study show that ixabepilone and paclitaxel accumulated in HCT116 cells (Figure 4 A and B, open symbols) however, ixabepilone accumulated more effectively in HCTVM46 compared to paclitaxel (Figure 4A and B, closed symbols). Thus, the ratios of drug concentrations in HCT116 versus HCTVM46 cells at the end of the 2 hr incubation period were 48 and 4, respectively, for paclitaxel and ixabepilone, reflecting the decreased susceptibility of the latter compound to the efflux mechanism mediated by Pgp.

Figure 4.   Comparative paclitaxel and ixabepilone uptake in the paclitaxel-sensitive parent HCT116 human colon carcinoma cell line and the Pgp overexpressing, paclitaxel-resistant variant HCTVM46

Paclitaxel (panel A) and ixabepilone (panel B) uptake in the HCT116 (open symbols) and the Pgp overexpressing HCTVM46 (closed symbols) human colon carcinoma cell lines. Panel C. Uptake ratios in HCT116 versus HCTVM46 for paclitaxel (open symbols) and ixabepilone (closed symbols). Results were from Study No. BMSR-2377.

[Figure excerpted from Sponsor]

35

B. *In vitro* characterization of the Pat-7 human ovarian and Pat-21 human breast carcinoma cell lines

1. **Expression of Pgp and MRP1**
    The Table below shows that Pat-7 human ovarian and the Pat-21 human breast cancer cell lines demonstrated paclitaxel resistance both *in vitro* (Pat-7) and *in vivo* in mice. However, these tumor models remained sensitive to ixabepilone. The human ovarian cell line, A2780Tax, reported to contain a β-tubulin mutation, also exhibits resistance to paclitaxel *in vitro* and *in vivo* but sensitivity to ixabepilone. As shown in Figure 2 (see above), Pat-7 expressed a high level of MRP1 and an intermediate level of Pgp. Expressions of Pgp and MRP1 were not detected in Pat-21 or A2780Tax.

Table 2   **Comparative cytotoxicity of ixabepilone and paclitaxel in paclitaxel resistant human cancer cell lines harboring various mechanisms of drug resistance**

Cell Line	IC$_{90}$ (nM)		Fold Potency Difference (Ixabepilone/paclitaxel)
	Paclitaxel	Ixabepilone	
A2780S (paclitaxel sensitive)	9.7	6.9	1.4
Pat-7 (paclitaxel resistant, MDR and MRP1)	150	7.4	20.3

Data source: BMSR-306, BMSR-334, BMSR-365, BMSR-366, BMSR-386, BMSR-393, and BMSR-397

[Table excerpted from Sponsor]

2. **Tubulin mutation status**
    Tubulin M40 and B2 genes were sequenced for mutation. No mutation that resulted in a change in amino acid sequence was found for Pat-7, Pat-21, HCT116 or HCTVM46; an A364T mutation was observed in A2780Tax. The results of these studies were not submitted with this published report.

Appears This Way
On Original

2.6.2.4 Safety pharmacology

<u>Neurological effects</u>:
930014842: The Comparison of the Effects of Ixabepilone and Taxol on Peripheral Nerve Function in the Rat: Electrophysiologic Measures (Non-GLP)

Key study findings:
- Ixabepilone at the doses and for the period evaluated is neurotoxic as shown by a slowing of sensory and motor maximal nerve conduction velocity and a reduction in sensory and motor compound response amplitudes.
- The strongest altered nerve conduction was observed at the high dose of 2.0 mg/kg.
- Initial effects at the high-dose (2.0 mg/kg) were detected beginning at 16/17 days in the distal digital nerve, at 30/31 days in the mixed caudal nerve and at 44/45 days in the tibial motor nerve.
- The effects at the high-dose (2.0 mg/kg) were similar to those seen for the positive control of taxol (15 mg/kg).
- At the 6-week recovery time point, peripheral neuropathy was still present in the groups treated with taxol and ixabepilone (2.0 mg/kg). However, some evidence of recovery occurred in the lower dose groups and in all dose groups for tibial motor response.

The study examined if administration of ixabepilone alters the peripheral nerve responses in the rat (as measured by electrophysiologic techniques). The time course and dose relationship of ixabepilone-induced changes was also examined. The effects of ixabepilone and taxol were compared. Rats (6/sex/dose) were administered single doses of ixabepilone via IV infusion at 0, 0.1, 1 and 2 mg/kg/week. Taxol, which served as the positive control, was administered at a dose of 15 mg/kg/week. After drug administration, electrophysiologic measures were collected from all rats at baseline, Day16/17, Day 30/31, Day 44/45, and Day 58/59. A subset of rats (2/sex/dose) were taken off compound and re-tested after a period of 2 and 6 weeks off compound (Recovery 1 and Recovery 2, respectively) to evaluate "coasting" and possible restoration of function. Peripheral electrophysiologic endpoints that were measured include caudal nerve action potential, digital nerve action potential and tibial motor conduction. No deaths were observed in the study.

Results are summarized in the Sponsor's tables below.

Appears This Way
On Original

Table 1 lists the overall *p*-value (ANOVA) across all groups for each measure and time point during active treatment. Table 2 lists the means and standard deviations for each measure, at a representative time point and group.

Table 1 - Overall ANOVA during baseline and treatment periods						
Overall ANOVA	Caudal NCV	Caudal amplitude	Digital NCV	Digital amplitude	Tibial latency	Tibial amplitude
Baseline	0.357	0.736	0.227	0.412	0.230	0.847
16/17 days	0.196	0.094	0.018	0.830	0.142	0.855
30/31 days	0.000	0.011	0.013	0.625	0.105	0.587
44/45 days	0.000	0.000	0.008	0.080	0.000	0.561
58/59 days	0.000	0.000	0.006	0.017	0.016	0.000

Table 2.

Day 58/59 end of treatment	temp	Caudal Nerve				Tibial Nerve		Digital Nerve			
		onset latency-msec	amplitude uV	distance dist.-mm	NCV meters/sec	onset latency-msec	amplitude mV	onset msec	amplitude uV	distance dist.-mm	NCV meters/sec
Set 1	37.07	1.38	15.31	60.00	44.27	2.00	5.97	0.87	16.77	32.08	37.12
Taxol	0.38	0.19	6.18	0.00	5.31	0.18	0.68	0.05	5.62	1.29	2.01
Set 2	37.06	1.48	16.44	60.00	40.79	2.14	6.50	0.96	12.09	32.50	33.92
2.0 mg/kg	0.37	0.11	5.34	0.00	2.90	0.24	1.55	0.05	1.96	1.31	2.11
Set 3	37.09	1.34	31.25	60.00	44.87	2.01	7.01	0.88	19.39	32.08	36.74
1.0 mg/kg	0.49	0.09	12.56	0.00	2.85	0.23	1.63	0.05	4.35	0.90	2.34
Set 4	36.9	1.20	36.44	60.00	50.25	1.81	6.48	0.86	19.78	32.21	37.82
0.1 mg/kg	0.49	0.08	11.34	0.00	3.05	0.22	1.04	0.06	4.28	1.37	2.67
Set 5	37.15	1.15	42.27	60.00	52.15	1.93	8.59	0.86	18.87	32.08	37.21
Control	0.48	0.05	15.06	0.00	2.21	0.18	1.61	0.04	7.41	1.47	2.02
Recovery 1 two weeks off treatment	temp	Caudal Nerve				Tibial Nerve		Digital Nerve			
		onset latency-msec	amplitude uV	distance dist.-mm	NCV meters/sec	onset latency-msec	amplitude mV	onset msec	amplitide uV	distance dist.-mm	NCV meters/sec
Set 1	36.68	1.24	13.39	60.00	48.64	1.70	6.53	0.92	13.14	31.88	34.87
Taxol	0.10	0.05	7.55	0.00	1.92	0.10	2.66	0.04	4.94	0.63	1.18
Set 2	36.95	1.46	9.75	60.00	41.60	1.92	5.53	0.88	13.29	31.75	36.13
2.0 mg/kg	0.29	0.28	1.21	0.00	7.00	0.05	1.22	0.07	3.44	0.29	2.67
Set 3	37.23	1.25	28.93	60.00	48.53	1.86	5.37	0.88	18.71	31.25	36.65
1.0 mg/kg	0.10	0.14	2.64	0.00	5.29	0.19	1.47	0.05	8.56	0.50	2.08
Set 4	37.0	1.14	37.60	60.00	52.92	1.85	6.70	0.85	20.70	31.38	36.84
0.1 mg/kg	0.26	0.04	7.69	0.00	1.99	0.19	2.57	0.05	8.82	1.11	1.14
Set 5	37.28	1.03	38.09	60.00	58.44	1.71	6.81	0.83	18.65	31.13	37.74
Control	0.17	0.03	7.46	0.00	1.93	0.09	2.26	0.03	6.04	1.11	0.88

[Tables excerpted from Sponsor]

Appears This Way
On Original

<u>Cardiovascular effects</u>:

920009347: Effects on hERG current and rabbit Purkinje-fiber action potential (Non-GLP)

Key study findings:
- HERG and Purkinje-fiber action potential activity was weak when tested at the high dose of 30 μM.
- BMS-247550 is not suspected to cause HERG/IKr-mediated electrocardiographic effects at anticipated plasma concentrations in patients.

BMS-247550 was tested *in vitro* for its effects on potassium (HERG/IKr) channel currents and rabbit-Purkinje fiber action potential. In the HERG assay, BMS-247550 was administered to HEK293 cells at 10 and 30 μM using whole-cell patch-clamp techniques and effects were calculated by measuring inhibition of peak tail currents.

BMS-247550 was tested in Purkinje fibers in rabbit at doses of 3, 10, and 30 μM and action potentials were recorded using intracellular techniques. Action potential parameters measured included resting membrane potential, overshoot, maximal upstroke velocity, and time to 50% and 90% repolorization.

As shown in Figure 1, BMS-247550 inhibited HERG currents by 5.7±3.4% (n=3) and 13.5±6.5% (n=3) at 10 and 30 μM, respectively.
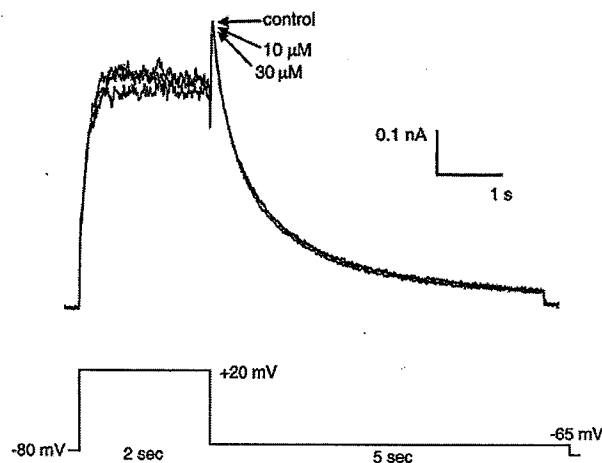
Figure 1. Effects of BMS-247550 on HERG currents expressed in an HEK293 cell. Currents were elicited by voltage steps (2 sec) applied at 10 second intervals from a holding potential of –80 mV to +20 mV. Tail currents were recorded at –65 mV. The percent inhibition of tail currents was used to calculate the % inhibition of HERG current since there are no endogenous tail currents in plasmid-transfected control HEK293 cells. Similar results were obtained in two additional cells.

As depicted in Table 1, BMS-247550 had minimal effects on Purkinje fiber on action activeial duration at 90% (APD$_{90}$), Vmax, overshoot (OS) and resting potential (RMP) at

all dose levels tested. BMS-247550 had slightly increased action potential duration at 90% (APD$_{50}$) at the high dose of 30 μM.

Conc. (μM)	Control	3	10	30
RMP (mV)				
Mean±sem	-87±1	-88±1	-87±1	-89±0
% Δ	0±0	2±1	0±1	3±1
OS (mV)				
Mean±sem	37±1	36±1	36±2	37±1
% Δ	0±0	-2±1	-1±4	2±1
Vmax (v/s)				
Mean±sem	499±10	496±15	493±14	508±13
% Δ	0±0	-1±1	-1±2	2±1
APD50 (ms)				
Mean±sem	150±13	154±13	157±20	178±10
% Δ	0±0	2±1	4±8	19±6
APD90 (ms)				
Mean±sem	259±12	258±10	259±11	260±11
% Δ	0±0	0±1	0±1	0±1

Table 1   Effects of BMS-247550 on action potential parameters

Pulmonary effects: No studies reviewed.

Renal effects: No studies conducted

Gastrointestinal effects: No studies conducted

Abuse liability: No studies conducted.

Other: No studies conducted.

2.6.2.5 Pharmacodynamic drug interactions

910074588: Pharmacodynamic and pharmacokinetic studies to determine the minimum effective exposure of BMS-247550 required for anti-tumor activity *in vivo*

This study was conducted to determine the minimum drug exposure required for BMS-247550 to produce anti-tumor activity using human ovarian carcinoma Pat-7 cell line. Results of these studies show the minimum effective concentration of BMS-247550 in systemic circulation of mice required for anti-tumor activity compared to the Pat-7 human ovarian carcinoma cell line was 30-90 nM for a total infusion of 10 hours.

The following outlines how the minimum infusional dose of BMS-247550 required for anti-tumor activity. This study was broken down into two parts.

1. In the first study, Pat-7 tumor bearing mice were administered BMS-247550 at doses of 18.8, 37.5, 75, and 150 mg/kg via constant rate IV infusion over a period of 10 hours. The result from this study show that all four dose levels were above

the minimum effective dose. The graph below that all four dose levels were similarly and significantly active yielding LCK values of 0.8, 1.1, 1.0, and 1.0 respectively.
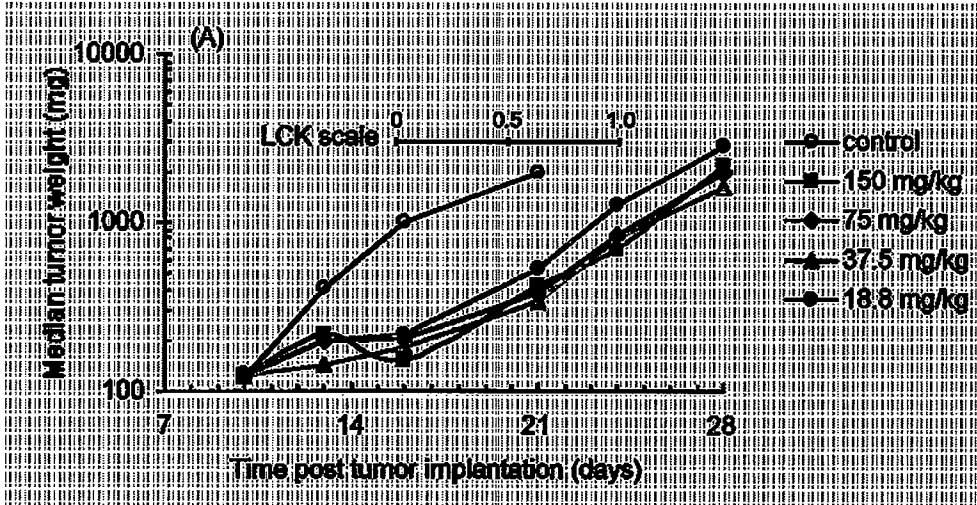
[Figure excerpted from Sponsor]

2. In the second study, Pat-7 tumor bearing mice were administered BMS-247550 at lower dose levels of 3, 6, 12, and 24 mg/kg via constant rate IV infusion over a period of 10 hours. Results from this study show that a clear dose response relationship was observed. The minimum effective dose (MED) required to produce anti-tumor activity equivalent to 0.5 log cell kill (LCK) was shown to be in the range of 3 to 6 mg/kg. The graph below shows that tumor growth delay equivalent to LCK values of 0.3, 0.6, 0.7, and 1.2 (corresponding to doses 3, 6, 12, and 24 mg/kg, respectively) with the last two values being statistically significant.

[Figure excerpted from Sponsor]

41
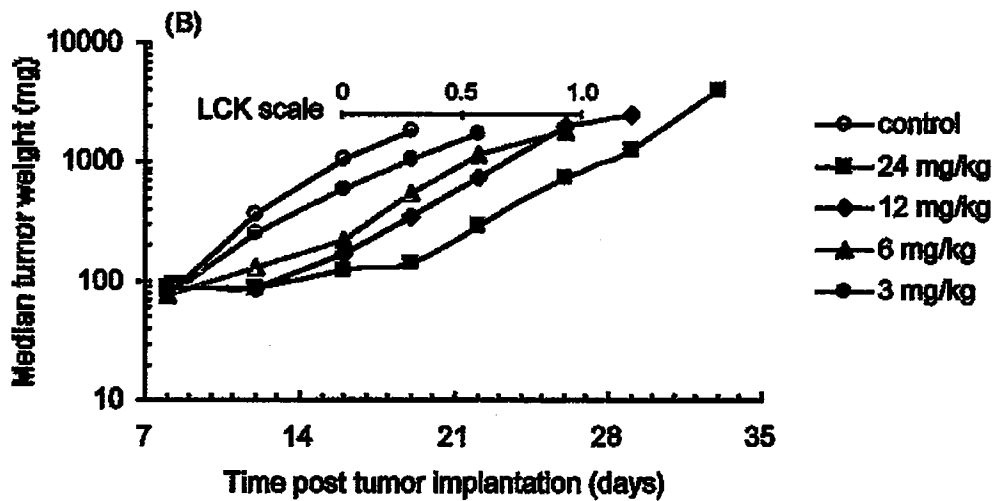
Two additional studies were conducted to determine the minimum effective drug exposure required for anti-tumor activity against Pat-7 human ovarian carcinoma.

1. In order to establish the minimal concentration of BMS-247550 needed for the first anti-tumor activity study, the plasma steady-state concentrations (Css) of BMS-247550 (achieved by a range of infusional dose levels) was obtained in non-tumor bearing mice. Once these values were determined, the pharmacokinetics of the drug given by prolonged constant rate infusion was characterized. The graph below shows plasma pharmacokinetics of infusional BMS-247550 in mice administered at a dose-rate of 4.5 mg/hr. Following the start of IV infusion, the concentration of BMS-247550 reached a steady-state level approximately 1-2 hours after the initiation of infusion.
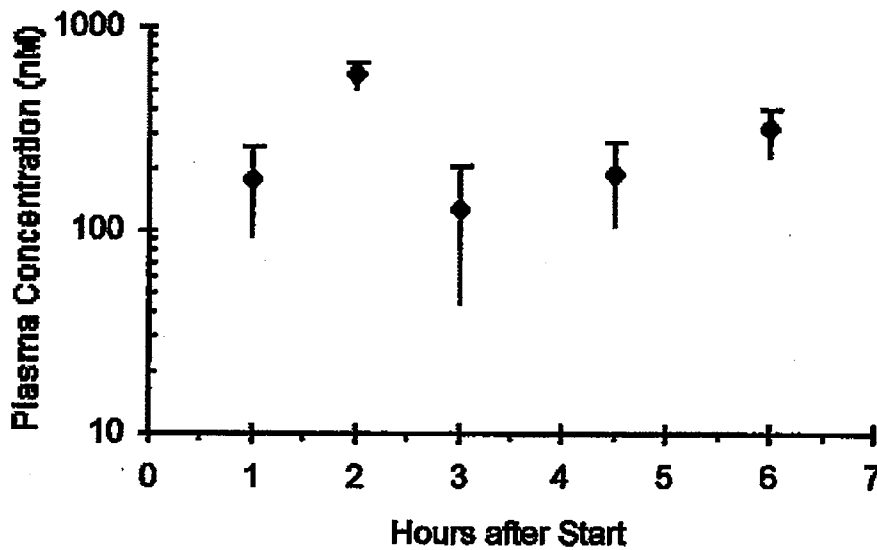
[Figure excerpted from Sponsor]

2. The steady state plasma concentration (Css) of BMS-247550 following infusion at various dose-rates ranging from 0.3-15 mg/kg/hr was determined. Css was calculated by taking the average of plasma concentrations at 2, 4 and 6 hours following the start of IV infusion. The graph below show the apparent Css achieved was proportional to dose over the entire dose-range evaluated.

**Appears This Way
On Original**

42
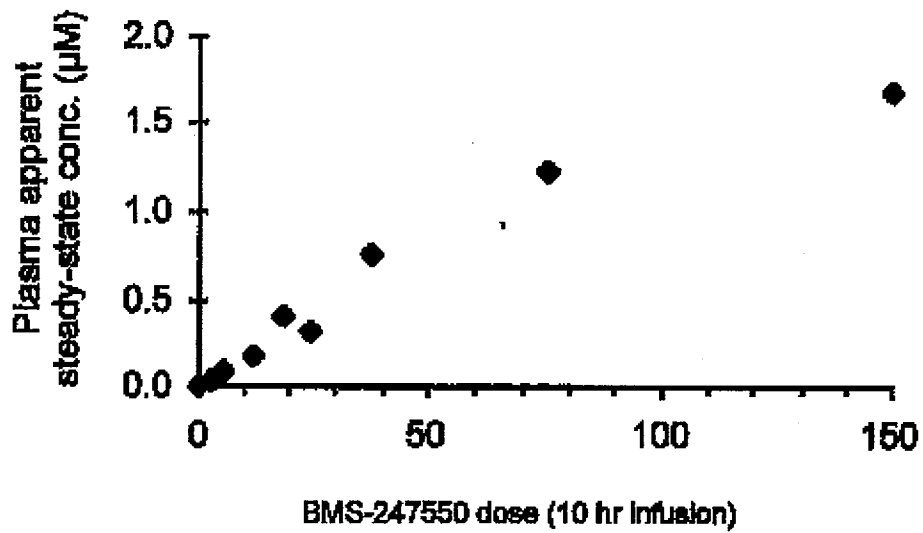
[Figure excerpted from Sponsor]

The graph below shows that Css at the minimum effective dose-range of 3-6 mg/kg were in the range of 0.03-0.09 uM (30-90 nM). This was defined as the minimum effective concentration (MEC) of the drug required for anti-tumor activity for the Pat-7 human ovarian carcinoma in mice.
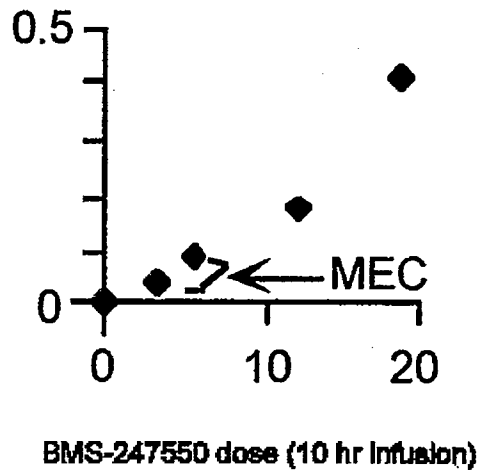
[Figure excerpted from Sponsor]

Appears This Way
On Original

2.6.3 PHARMACOLOGY TABULATED SUMMARY

Summary of the Mechanism and Significant Findings of Ixabepilone		
Type of study	**Test system**	**Significant findings**
Primary pharmacodynamics		
Tubulin dynamics	Pat-21(Human breast cancer model derived from a tumor completely refractory to paclitaxel)	Analysis of the β-tubulin isoform composition of the Pat-21 model reveals expression of βII (1-13%) and absence of βII.
Tubulin binding	Isolated bovine brain β tubulin	Using isothermal titration calorimetry (ITC), ixabepilone was found to bind pre-formed microtubules with an average apparent dissociation constant of 220 nM.
Microtubule dynamic instability	Isolated and purified βII and βIII-tubulins	1. Ixabepilone (at 25nM) produced equivalent suppression of mictrotubule dynamicity (40-50%) as paclitaxel (250nM). 2. Ixabepilone had suppressive effect on dynamic instability of αβ-II or αβ-III microtubules. Paclitaxel was only effective in suppressing the dynamic instability of αβ-II microtubules.
Further studies on preclinical pharmacology	1. Cell line panels consisting of breast (35 lines), colon (20 lines) and lung (23 lines) 2. Pat-21 tumor (human paclitaxel resistant breast carcinoma); 16C/ADR and MCF7/ADR (Pgp positive, multidrug resistant breast cancer models) 3. Combination studies with ixabepilone and approved anticancer agents when administered at MTD 4. 35 human tumor xenografts (8 breast, 4 NSCLC, 4 pancreatic, 8 ovarian, 4 prostate, 4 colon, 1 SCLC, 1 gastric, and 1 SCC)	1. Ixabepilone showed cytotoxicity against breast (IC_{50} 1.4-45nM), colon (IC_{50} 4.7-42nM) and lung cancer cell lines (IC_{50} 2.3-19nM). 2. In Pat-21 model, ixabepilone had significant antitumor activity (LCK=1.6) compared to doxetaxel (LCK=0.2). In 16C/ADR model, tumors was significantly less responsive to adriamycin (0.5 versus >3.7 LCK) and paclitaxel (1.4 versus 2.6 LCK) but remained highly sensitive to ixabepilone (3.5 versus >3.7 LCK). In MCF7/ADR model, ixabepilone had antitumor activity (LCK=0.5) compared to paclitaxel (LCK=0). 3. Significant effects with capecitabine, cetuximab, bevacizumab, and trastuzumab; modest effects with irinotecan; no difference with gefitinib, paclitaxel, irinotecan and gemcitabine. 4. Ixabepilone showed antitumor activity against 33 of 35 human tumor xenografts with prolonged tumor growth delay to or greater than 1 LCK.
Cytotoxicity	Human tumor cell line (breast, prostate, lung, colon, ovarian, and leukemia)	Four ixabepilone degradants were less cytotoxic *in vitro* (39 to >312-fold) than ixabepilone.
Secondary pharmacodynamics		
Cellular drug accumulation in a MDR cell line that efficiently efflux paclitaxel from cells.	Human colon (HCTVM46), human ovarian (Pat-7), and human breast carcinoma (Pat-21) cell lines	Ixabepilone had significant accumulation in HCTVM46 cells, resulting in a ~10-fold accumulation in cells (intracellular/extracellular). In contrast, paclitaxel accumulated by only 2-fold during the same period.
Pharmacodynamic drug interactions		
PD and PK studies to determine effective exposure	Pat-7 tumor bearing mice	In human ovarian cancer model derived from a patient who developed resistance to paxlitaxel, the minimum effective concentration required to produce antitumor activity was in the range of 30-90 nM.

Appears This Way
On Original

2.6.4   PHARMACOKINETICS/TOXICOKINETICS

2.6.4.1 Brief summary

The pharmacokinetic behavior of ixabepilone was examined in all the non-clinical species tested for toxicity. In rats and dogs, systemic exposure of ixabepilone was dose-related, with no gender related difference. In rat 9-month studies, however, male rats appeared to have higher Cmax levels compared to female rats at high dose levels. No accumulation was observed. after intermittent repeated dosing, but 2 to 3 fold accumulation was generally observed after daily repeated dosing to rats and dogs.

The metabolic profile of ixabepilone is very similar across species; mouse, rat, dog, and human. Metabolites of ixabepilone identified in rat, dog, and human were products of oxidative biotransformation. Major metabolites in rat and dogs (also detected in liver microsomes in mouse, rat, dog, monkey, and human) included M8 (M+16 metabolite), M41 (M+16 metabolite), and M19 (M-2 metabolite). Major degradants include BMS-249798, BMS-326412 —————— which were detected in the plasma, urine, and feces of rats and dogs. The metabolite and degradant profile in rats and dogs plasma are similar with unchanged ixabepilone being the most abundant drug-related component. Metabolites, formed from the hepatic metabolism of ixabepilone, did not appear to contribute to the drug's overall toxicity when tested against a human colon carcinoma line.

In vitro studies indicate that metabolism of ixabepilone involves P450 isozymes CYP3A54 and CYP3A5. Ixabepilone was shown not to cause an increase in enzyme activity or the mRNA-expression of CYP1A2, CYP2B6, CYP2C9, or CYP3A4 in primary human hepatocyte cultures. Ixabepilone was shown not to inhibit activities of CYP enzymes 1A2, 2A6, 2B6, 2C8, 2C9, 2C19, 2D6, and 2E1 in human liver microsomes (HLM), but inhibited CYP3A4 in a metabolism-dependent manner.

In mouse, rat, and dog, ixabepilone has a moderate to high clearance. Metabolism plays a major role in the elimination of the drug in all species. Following an IV dose, ixabepilone-derived radioactivity is primarily excreted in the feces (>64%) in rats and dogs while a small amount (<22%) of the drug is excreted in the urine. In studies with bile duct-cannulated rats, the ixabepilone-derived radioactivity is excreted in the bile (53%) and urine (15%). In bile duct-cannulated rats, unchanged parent drug represented <1% of the dose in bile and approximately 2% of the dose in urine. In intact rats and dogs, only a small fraction of the radioactivity in feces (≤2.1%) and urine (<3%) was attributed to the parent compound.

2.6.4.2 Methods of Analysis

[see under individual study reviews]

Appears This Way
On Original

2.6.4.3 Absorption
MAP005/247550-910074578: Preliminary evaluation of the pharmacokinetics and metabolism of BMS-247550

Mice, rats and dogs were given different administrative routes of BMS-247550 and the pharmacokinetics was determined. In all three species, BMS-247550 was rapidly cleared, had a high volume of distribution, and a long elimination half-life. Oral bioavailability in mice and in the rats was= 7.5% and the mouse was = 31.0%. Intraduodenal bioavailability in rats was higher compared to oral (27.0% compared to 7.5%) due to poor stability of drug at low pH.

Species	Route, dose	N=	C_{MAX} (ng/mL)	AUC(INF) (ng.h/mL)	$t_{1/2}$ (hr)	Cl (mL/min/kg)	V_{ss} (L/kg)	F (%)
Rat	IA, 2 mg/kg	6	—	648	9.6	56	23	—
	PO, 8 mg/kg	3	228	194	—	—	—	7.5
	ID, 8 mg/kg	3	642	697	—	—	—	27
Mouse	IV, 5 mg/kg	—	—	1227	≈3	68	6.3	—
	PO, 48 mg/kg*	—	5983	3640	—	—	—	31
Dog	IV, 0.5 mg/kg	3	—	483	≈24	17	25	—

*buffered solution.

[Table excerpted from Sponsor]

Additional studies were conducted with the following results (No additional data was provided in study report):

- *In vitro* liver microsomes studies (rat, dog or human) suggest chemical degradation is the main clearance pathway of BMS-247550.
- Rat and dog plasma studies suggest that BMS-247550 appears to be somewhat more stable in plasma compared to buffer.
- *In vitro* metabolism studies with BMS-27450 and recombinant human CYP isoforms found is a weak inhibitor of human CYP3A4 with an average IC_{50} of 7.3uM. When BMS-247550 was incubated with human liver microsomes along with compounds specific for the inhibition of individual cytochrome P450's, significant inhibition was found with CYP3A4 inhibitors. Thus, in humans BMS-247550 may be a potential substrate for CYP3A4 *in vivo*.

2.6.4.4 Distribution
930011862: *In vitro* determination of serum protein binding and blood cell distribution of ixabepilone (BMS-247550) in mouse, rat, dog and human

The *in vitro* serum protein binding and blood cell distribution of ixabepilone in mouse, rat, dog and human over the concentration range of 50 to 5000 ng/mL was determined. The concentrations of ixabepilone in serum and ultrafiltrate (for protein binding) and plasma (for blood cell distribution) were measured by LC/MS/MS. The mean percent of free drug in serum ranged from 17.9 to 56.4%, 9.1 to 40.2% and 23.4 to 32.9% in rat, dog and human serum, respectively. The percent of free drug in mouse serum at the highest concentration was 7.6% at 5000 ng/mL concentration. The extent of serum protein

binding decreased with increasing concentration over the concentration range of 50 to 5000 ng/mL. The mean blood to plasma ratios ranged from 0.76 to 0.96, 1.30 to 12.97, 0.75 to 4.25, and 0.65 to 0.85 in mouse, rat, dog and human, respectively. Overall, ixabepilone is extensively bound in mouse serum proteins (92.4% at 5000 ng/mL) and is moderately bound in rat, dog and human serum proteins. Ixabepilone showed moderate distribution into blood cells except high distribution at the nominal concentration of 50 ng/mL in rat and dog.

The mean results (SD) are summarized in the table below.

Nominal Concentration (ng/mL)	Percent bound to serum proteins, Mean (SD)				Percent distribution into blood cells, Mean (SD)			
	Mouse	Rat	Dog	Human	Mouse	Rat	Dog	Human
50	ND[a]	82.1 (0.9)	90.9 (1.2)	76.6 (1.9)	13.1 (1.0)	95.6[b]	90.2 (1.8)	12.6 (4.5)
500	ND[a]	77.8 (1.4)	86.9 (1.4)	72.0 (1.7)	13.8 (3.8)	60.0 (9.1)	46.2 (3.2)	21.6 (3.4)
5000	92.4 (0.5)	43.6 (3.9)	59.8 (0.6)	67.1 (1.9)	31.2 (1.4)	54.7 (1.6)	45.8 (1.8)	33.6 (3.6)

[a] ND: not determined. Ixabepilone concentration recovered in the ultrafiltrate that represents free concentration was less than LLQ. Therefore, the percent bound to serum protein could not be determined.
[b] N=2, no SD reported.

[Table excerpted from Sponsor]

————————————————/930009762: Tissue Distribution and Excretion of Total Radioactivity Following Intravenous Administration of [^{14}C] BMS-247550 to Male and Female Long-Evans Rats – Tissue Distribution Report

The tissue distribution of radioactivity was examined following administration of a single intravenous dose of [^{14}C] BMS-247550 at 2.75 mg/kg to male and female rats. Groups 1 and 4, one animal/sex, served as controls for blood collection. In Group 2, blood was collected from three animals/sex/time point at 0.5, 1, 4, 8, 24, 48, 72, and 168 hours postdose and in Group 3 blood was collected from three animals/sex/time point at 1, 4, 8, and 24 hours postdose (for biotransformation study). Following blood collection, the Group 2 animals were sacrificed and selected tissues collected. Blood, plasma, and tissues were analyzed for total radioactivity.

Distribution of radioactivity:
The distribution of radioactivity was quantifiable in all analyzed tissues at 0.5 and 1 hour postdose in both males and females. Radioactivity reached maximum concentrations at 0.5 and 1 hour for all tissues except large intestine, eye lens, and thymus. Levels of radioactivity decreased slowly with time and at 168 hours postdose, radioactivity was still quantifiable in all tissues except cerebrospinal fluid, esophagus, plasma, and spinal cord in males and females and cerebellum in males.

Mean concentrations of radioactivity and Cmax concentrations:
The maximum mean concentrations of radioactivity in blood and plasma for Group 2 animals were 1,160 and 1,440 ng equivalents [^{14}C] BMS-247550/g, respectively, in males, and 1,410 and 1,650 ng equivalents [^{14}C] BMS-247550/g, respectively, in females at 0.5 hours postdose. The tissues with the highest mean Cmax concentrations were small intestine, pituitary gland, bone marrow, liver, adrenal glands, and lungs in males

and females, spleen and kidneys in males, and thyroid/parathyroid and thymus in females. The tissues with the lowest Cmax concentrations of radioactivity were the eye lens, cerebrospinal fluid, and spinal cord.

Concentrations of radioactivity for pigmented and non-pigmented skin:
The concentrations of radioactivity for pigmented and non-pigmented skin were similar at all collection time points in both males and females. The Cmax concentration in pigmented eyes was moderate at 1 hour postdose in males and females and declined slowly through the end of the study. These data suggest [^{14}C] BMS-247550-derived radioactivity does not bind to melanin. Low levels of [^{14}C] BMS-247550-derived radioactivity were observed in the cerebellum, spinal cord, and testes, suggesting that the drug-derived radioactivity crossed the blood/brain and blood/testes barriers.

Tissue:plasma ratios:
The tissue:plasma ratios were greater than one for nearly all tissues where radioactivity was detected in both sexes. The highest tissue:plasma ratios were observed in thymus and pituitary gland at 72 hours postdose with values of 333 and 149, respectively, in males and 506 and 169, respectively, in females.

Tissues with radioactivity:
Most of the dosed radioactivity was found in liver, muscle, nonpigmented skin, pigmented skin, small intestinal contents/wash, and large intestinal contents/wash. The amount of radioactivity in the small intestinal contents/wash and large intestinal contents/wash observed with time suggests biliary excretion of drug-derived radioactivity and the transit of the radioactivity through the gastrointestinal (GI) tract. The maximum mean concentration of radioactivity in blood and plasma in Group 3 animals occurred at 1 hour postdose with mean values of 885 and 1,180 ng equivalents [^{14}C] BMS-247550/g, respectively, in males and 1,130 and 1,370 ng equivalents [^{14}C] BMS-247550/g, respectively, in females. Plasma concentrations declined with time to 49.9 and 39.4 ng equivalents [^{14}C] BMS-247550/g at 24 hours postdose, respectively, in males and females.

Conclusions:
Overall, there were no notable gender differences in the mean concentrations of [^{14}C] BMS-247550/g-derived radioactivity in blood, plasma, and tissues. [^{14}C] BMS-247550-derived radioactivity was extensively distributed in the tissues with the tissue:plasma ratios greater than one for most tissues in both sexes.

—————————————'930010650: Lacteal Excretion and Fetal Tissue Distribution of Radioactivity in Pregnant Female Sprague Dawley Rats and Tissue Distribution of Radioactivity in Male and Non-Pregnant Female Sprague Dawley Rats Following Intravenous Administration of [^{14}C]BMS-247550

The tissue distribution and lacteal excretion of [^{14}C]BMS-247550-derived radioactivity was assessed following an intravenous administration of [^{14}C]BMS-247550 at a dose of 2.75 mg/kg to timed-pregnant female, non-pregnant male and female rats. Control blood, milk, and tissues were collected (Groups 1 and 2). Blood and selected tissues were collected (Group 3, GD 18) at 0.1, 0.5, 1, 3, 6, 12, 24, 48, and 72 hours postdose to examine the tissue distribution of [^{14}C]BMS-247550-derived radioactivity in maternal and fetal tissues. Milk, blood, and plasma were collected (Group 5, 7-9 days postpartum)

at 0.1, 0.5, 1, 3, 6, 12, 24, 48, and 72 hours postdose to assess the lacteal excretion of [^{14}C]BMS-247550-derived radioactivity. One animal/time point (Group 4, GD Day 18) was sacrificed at 0.1, 0.5, 1, 3, 6, 12, 24, 48, and 72 hours postdose; and 1 animal/sex/time point (Group 6, non-pregnant females and males) was sacrificed at 0.1, 0.5, 1, 3, 6, 12, 24, 96, and 168 hours post-dose to examine tissue distribution of radioactivity by whole-body autoradiography (WBA).

Results were as follows (Also see Sponsor's tables below):
- At GD 18, the terminal $t_{1/2}$ values for radioactivity in maternal blood, maternal plasma, and fetal blood were 39.6, 33.3, and 13.1 hours, respectively in pregnant rats.
- [^{14}C]BMS-247550-derived radioactivity was distributed in maternal and fetal tissues, with maximum concentrations occurring at 0.1 and 0.5 hours post-dose for maternal tissues and amniotic fluid and at 0.1 to 6 hours post-dose for all fetal tissues.
- [^{14}C]BMS-247550-derived radioactivity crossed the placenta and the blood/brain barrier at low levels in pregnant rats dosed on GD 18.
- Concentrations of [^{14}C]BMS-247550-derived radioactivity in maternal blood, liver, and kidneys were higher than the equivalent fetal tissues at all time points except fetal liver at 3 hours post-dose and kidneys at 24 hours postdose. Concentrations in fetal brain were higher than maternal cerebrum in all time points.
- [^{14}C]BMS-247550-derived radioactivity was excreted in milk, with radioactivity detected at all time points through 72 hours postdose. The milk:plasma concentration ratios ranged from 0.296 to 2.64.
- [^{14}C]BMS-247550-derived radioactivity was extensively distributed in male and non-pregnant female tissues. There were no apparent gender differences in the tissue concentration data.

Appears This Way
On Original

Table 5
Mean (SD) concentrations of radioactivity in maternal blood, plasma, and tissues,
and fetal blood and tissues at specified times following an intravenous
administration of [^{14}C]BMS-247550 (2.75 mg/kg) to pregnant female rats
(Gestation Day 18, Group 3)

| | ng Equivalents [^{14}C]BMS-247550/g | | | | | | | |
| | 0.1 Hour | | 0.5 Hour | | 1 Hour | | 3 Hours | |
Matrix	Mean	SD	Mean	SD	Mean	SD	Mean	SD
Amniotic fluid	23.2	10.0	82.4	5.5	74.8	12.7	79.7	20.7
Blood	2400	130	1300	80	643	44	215	35
Cerebrum	209	30	146	16	108	10	83.0	6.5
Heart	5050	220	3690	50	2760	120	2070	90
Kidneys	6810	110	6580	90	5700	60	4560	120
Liver	10000	300	7310	350	6230	270	4430	180
Lungs	5090	900	4360	770	3960	600	4510	40
Ovaries	5170	200	5180	160	4160	270	2560	140
Placenta	3010	90	3260	30	3170	120	2750	200
Plasma	2750	210	1500	100	801	43	250	53
Uterus	2960	120	3890	80	3510	90	3360	320
Fetal blood	236	41	226	41	181	25	100	15
Fetal brain	273	74	322	57	317	37	412	82
Fetal carcass	528	105	829	182	948	99	1380	250
Fetal kidneys	1830	360	2740	390	2820	190	3120	640
Fetal liver	1870	160	3620	450	4170	450	4570	390

SD   Standard deviation.

Note: Each value represents the mean of 3 animals for maternal matrices and the mean of 6 fetuses
       (2/dam) for fetal tissues.

Table 5 (continued)
Mean (SD) concentrations of radioactivity in maternal blood, plasma, and tissues
and fetal blood and tissues at specified times following an intravenous
administration of [^{14}C]BMS-247550 (2.75 mg/kg) to pregnant female rats
(Gestation Day 18, Group 3)

| | ng Equivalents [^{14}C]BMS-247550/g | | | | | |
| | 6 Hours | | 12 Hours | | 24 Hours | |
Matrix	Mean	SD	Mean	SD	Mean	SD
Amniotic fluid	56.0	4.0	25.3	0.6	18.9	3.6
Blood	140	16	79.4	6.1	47.7	10.8
Cerebrum	79.5	11.4	77.0	10.8	66.3	5.0
Heart	1800	10	1450	50	987	96
Kidneys	3740	60	2920	120	1950	220
Liver	3700	50	2970	40	1770	470
Lungs	3120	630	2680	640	2000	200
Ovaries	2120	60	1130	960	1360	150
Placenta	2350	190	2120	60	1580	170
Plasma	162	24	94.5	1.3	50.8	15.4
Uterus	2640	280	2370	70	2000	80
Fetal blood	98.4	26.7	55.9	5.9	36.3	20.1
Fetal brain	447	94	444	45	403	104
Fetal carcass	1570	160	1250	130	873	129
Fetal kidneys	3420	460	2770	330	2080	560
Fetal liver	3540	410	2560	120	1310	240

SD   Standard deviation.

Note: Each value represents the mean of 3 animals for maternal matrices and the
       mean of 6 fetuses (2/dam) for fetal tissues.

Appears This Way
On Original

Table 5 (continued)
Mean (SD) concentrations of radioactivity in maternal blood, plasma, and tissues,
and fetal blood and tissues at specified times following an intravenous
administration of [^{14}C]BMS-247550 (2.75 mg/kg) to pregnant female rats
(Gestation Day 18, Group 3)

Matrix	ng Equivalents [^{14}C]BMS-247550/g			
	48 Hours		72 Hours	
	Mean	SD	Mean	SD
Amniotic fluid	16.6	1.8	15.4	5.8
Blood	25.7	1.9	20.6	1.7
Cerebrum	63.6	8.0	57.2	7.8
Heart	618	70	419	63
Kidneys	1120	150	868	124
Liver	1190	240	945	181
Lungs	1140	120	853	95
Ovaries	795	25	639	78
Placenta	1150	40	931	70
Plasma	23.3	0.6	18.7	2.8
Uterus	1540	70	1430	130
Fetal blood	8.67	10.1	0.00	0.00
Fetal brain	306	60	230	31
Fetal carcass	482	61	348	52
Fetal kidneys	1280	340	758	179
Fetal liver	392	107	225	37

SD   Standard deviation.

Note: Each value represents the mean of 3 animals for
         maternal matrices and the mean of 6 fetuses (2/dam)
         for fetal tissues.

Table 16
Mean (SD) blood:plasma and milk:plasma concentration ratios at specified times
following an intravenous administration of [^{14}C]BMS-247550 (2.75 mg/kg) to
lactating female rats (Day 7 to 9 Postpartum, Group 5)

Collection Time (Hours)	Concentration Ratios	
	Mean	SD
	Blood:Plasma	
0.1	0.870	0.058
0.5	0.888	0.036
1	1.01	0.33
3	0.906	0.084
6	0.846	0.220
12	1.12	0.09
24	1.10	0.02
48	1.13	0.07
72	1.49	0.28
	Milk:Plasma	
0.1	0.296	0.129
0.5	0.963	0.069
1	0.805	0.496
3	0.483	0.032
6	0.512	0.052
12	1.15	0.21
24	1.24	0.08
48	2.64	1.62
72	1.27[a]	NA

NA   Not applicable.
SD   Standard deviation.

Note: Each value represents the mean of 3 animals.

a   Value represents the average of 2 animals.

_4_ Page(s) Withheld

_X_ Trade Secret / Confidential

_____ Draft Labeling

_____ Deliberative Process

Withheld Track Number: Pharm/Tox-_____

2.6.4.5 Metabolism

930009177: Comparative *in vitro* biotransformation of [^{14}C] ixabepilone (BMS-247550) in liver microsomal preparations of mice, rats, dogs, monkeys and humans

Comparative *in vitro* biotransformation profiles of ixabepilone were determined using liver microsomal preparations from mice, rats, dogs, monkeys and humans. 20 µM of [^{14}C] ixabepilone was incubated with liver microsomal preparations at two time-points (0.5 and 1 hour). At the end of the incubation period, acetonitrile was added to terminate the reaction and to extract drug-related compounds. The extracts were analyzed by HPLC and LC/MS. Results showed that metabolism of [^{14}C] ixabepilone in mouse, rat, dog, monkey and human liver microsomes incubations was moderate to extensive. The rank of metabolic stability was the following: mouse=monkey=human>rat>dog (Table 2). Table 2 also shows that after 1 hour of incubation, unchanged ixabepilone (BMS-247550) accounted for 12, 43, 60, 10 and 15% of radioactivity in liver microsomes from mouse, rat, dog, monkey and human, respectively.

Table 2:   Percent distribution of [^{14}C]ixabepilone and its metabolites after a 1-hour incubation with liver microsomes from mice, rats, dogs, monkeys and humans

Peak ID [a]	R$_t$ (min) [b]	Metabolite Distribution (% of Radioactivity)				
		Mouse	Rat	Dog	Monkey	Human
M1		7%	5%	2%	5%	3%
M2		3%	1%	1%	2%	1%
M3		0.4%	ND[c]	ND[c]	ND[c]	1%
M4		1%	2%	3%	ND[c]	1%
M5		ND[c]	1%	1%	2%	1%
M6		ND[c]	1%	1%	ND[c]	1%
M7		7%	1%	1%	5%	3%
M8		24%	15%	7%	18%	15%
M9-M15 [d,e]		4% (M9) / 10% (M10-M15)	5% (M9) / 5% (M10-M15)	5%	18%	13%
M16-M17 [d]		3%	2%	1%	4%	7%
M18		1%	1%	ND[c]	2%	3%
M19		2%	1%	1%	2%	3%
M20		2%	2%	2%	3%	4%
BMS-247550		12%	43%	60%	10%	15%
BMS-249798		1%	4%	6%	ND[c]	2%
Total [f]		77.4%	89%	91%	71%	73%

[a] M1 to M20: radioactive metabolite peaks detected and characterized in the *in vitro* incubations.
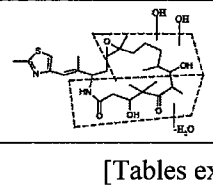
[b] R$_t$: HPLC retention time

[c] ND: Not detected
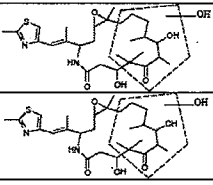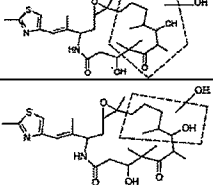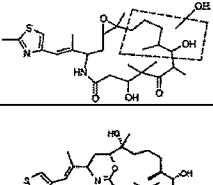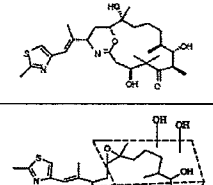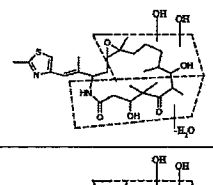
[d] Peaks co-eluted and were integrated as one. M9 was well separated from other metabolites only in mouse and rat microsomes.

[e] M9 in monkey microsomes, M10 in rat microsomes and M12 in mouse microsomes were not detected by LC/MS analysis.

[f] Total includes only the characterized metabolites. The remaining radioactivity was distributed over the HPLC region between ~15 to 50 min without any distinctive peaks.
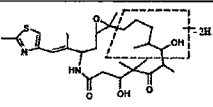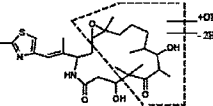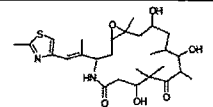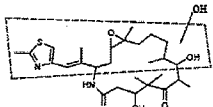
[Table excerpted from Sponsor]
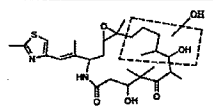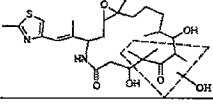
A total of 20 metabolites and one degradation product (BMS-249798) were identified from the five species tested. In all five species, [14C] ixabepilone is metabolized mainly by oxidation resulting in the formation of M+16, M+14 and M-2 metabolites. The main metabolites in human liver are M8, M19 and M20. M8 and M20 are identified as a hydroxylated and keto metabolite, respectively. Of the twenty metabolites detected in the human preparations, sixteen were detected in the monkey preparations, seventeen were detected in mouse, eighteen were detected in rat, and eighteen were detected in the dog preparations showing that the metabolism of [14C] ixabepilone is similar in humans and the animal species. The metabolites and their structures are shown in Table 3. Figure 28 shows the proposed biotransformation of [14C] ixabepilone in liver microsomes.

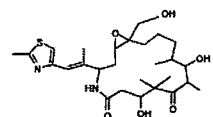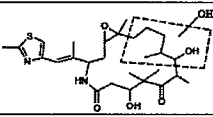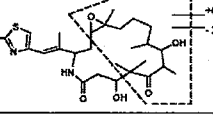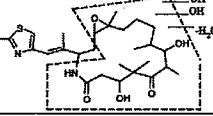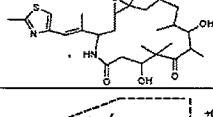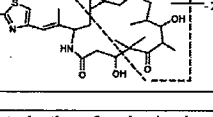| Table 3:			LC/MS characterization of major in vivo metabolites of ixabepilone	
Peak[a]	[M+H][+]	Major Fragment Ions	Chemical Structure	Species Found
M1	523	505, 487, 469, 418, 400, 382, 318, 237, 166		MLM, RLM, DLM, MKLM, HLM
M2	523	505, 487, 469, 400, 382, 237		MLM, RLM, DLM, MKLM, HLM
M3	523	505, 487, 436, 418, 400, 382, 336, 318, 300, 236, 237		MLM, HLM
BMS-249798	507	166, 237, 302, 320, 337, 384, 402, 420, 471, 489		MLM, RLM, DLM, HLM
M4	521	503, 485, 352, 334, 218, 166		MLM, RLM, DLM, HLM
M5	521	503, 352, 334, 316, 298, 236, 218, 166		RLM, DLM, MKLM, HLM

[Tables excerpted from Sponsor]
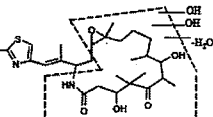
Appears This Way
On Original

Table 3:		LC/MS characterization of major in vivo metabolites of ixabepilone		
Peak[a]	[M+H]+	Major Fragment Ions	Chemical Structure	Species Found
M6	505	487, 469, 418, 400, 318, 237, 166		RLM, DLM, HLM
M7	521	503, 485, 434, 416, 166		MLM, RLM, DLM, MKLM, HLM
M8	523	505, 487, 469, 436, 418, 400, 382, 336, 318, 300, 237, 236, 218, 166		MLM, RLM, DLM, MKLM, HLM
M9	523	505, 487, 436, 418, 400, 336, 318, 300		MLM, RLM, DLM, HLM
M10	523	505, 487, 436, 418, 400, 336, 318, 236		MLM, DLM, MKLM, HLM
M11	523	505, 436, 418, 400, 320, 302, 166		MLM, RLM, DLM, MKLM, HLM

[Tables excerpted from Sponsor]
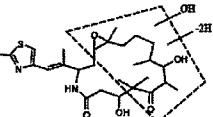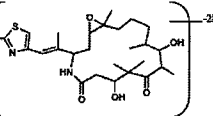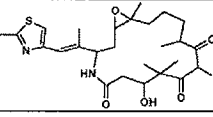
Appears This Way
On Original

Table 3: LC/MS characterization of major in vivo metabolites of ixabepilone

Peak[a]	[M+H]+	Major Fragment Ions	Chemical Structure	Species Found
M12	523	505, 487, 436, 418, 400, 336, 253, 166		RLM, DLM, MKLM, HLM
M13	523	505, 487, 436, 418, 400, 336, 318, 237		MLM, RLM, DLM, MKLM, HLM
M14	521	503, 485, 434, 336, 318, 300, 166		MLM, RLM, DLM, MKLM, HLM
M15	521	503, 485, 352, 334, 316, 166		MLM, RLM, DLM, MKLM, HLM
Ixabepilone (BMS-247550)	507	489, 471, 420, 402, 384, 320, 302, 237, 166		MLM, RLM, DLM, MKLM, HLM
M16	521	503, 485, 336, 318, 300, 166		MLM, RLM, DLM, MKLM, HLM

Table 3: LC/MS characterization of major in vivo metabolites of ixabepilone

Peak[a]	[M+H]+	Major Fragment Ions	Chemical Structure	Species Found
M17	521	503, 485, 352, 334, 166		MLM, RLM, DLM, MKLM, HLM
M18	521	503, 485, 336, 318, 300, 166		MLM, RLM, MKLM, HLM
M19	505	487, 336, 318, 300, 166		MLM, RLM, DLM, MKLM, HLM
M20	505	505, 487, 469, 418, 400, 336, 318, 237, 166		MLM, RLM, DLM, MKLM, HLM

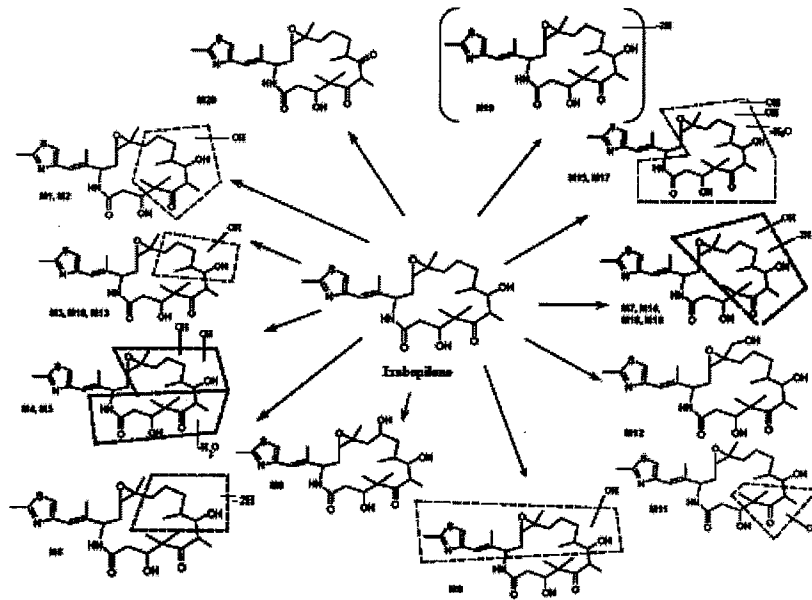[a] Peak designations are shown in Figure 2.
LC/MS/MS was performed in the positive ion mode.
MLM: mouse liver microsome; RLM: rat liver microsome; DLM: dog microsome; MKLM: monkey liver microsome; HLM: human liver microsome

[Tables excerpted from Sponsor]

Figure 28:   Proposed biotransformation of [^{14}C]ixabepilone in liver microsomes
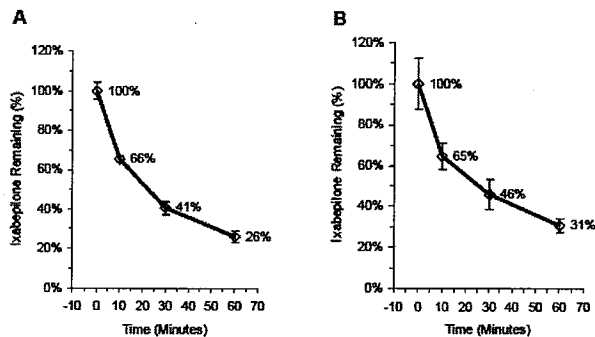

[Figure excerpted from Sponsor]

Appears This Way
On Original

930019253: Evaluation of the *in vitro* cytotoxicity of a mixture of metabolites of ixabepilone (BMS-247550), which were generated in human liver microsomes, against a human colon carcinoma cell line

A mixture of ixabepilone and its metabolites in human liver microsomes was examined to evaluate it cytotoxicity when incubated in human tumor cells. 10 µM of ixabepilone was incubated with liver microsomal preparations at different time-points (0, 10, 30 and 60 min). At the end of the incubation period, ethanol was added to the mixture to terminate the reaction and extract drug-related compounds. The ethanol extracts were analyzed by LC/MS to determine the concentration of ixabepilone at various timepoints and to evaluate the metabolites. After a 1-hour incubation period, the following oxidative metabolites were identified: M2, M3, M4, M5, M8, M10, M11, M12, M13, M14, M15, M16, M17, M19 and M20.

Analysis of the microsomal mixtures following varying time of incubation showed a time-dependent loss of ixabepilone from the mixtures. Figures 1A and 1B show that in two separate studies, the trend of time-dependent loss (sampled at 0, 10, 30 and 60 min.) of the parent compound was reproducible.

Figure 1:   **Stability of ixabepilone in human microsomal mixtures. (A) Study No. BMSR-2433 and (B) Study No. BMSR-2506**
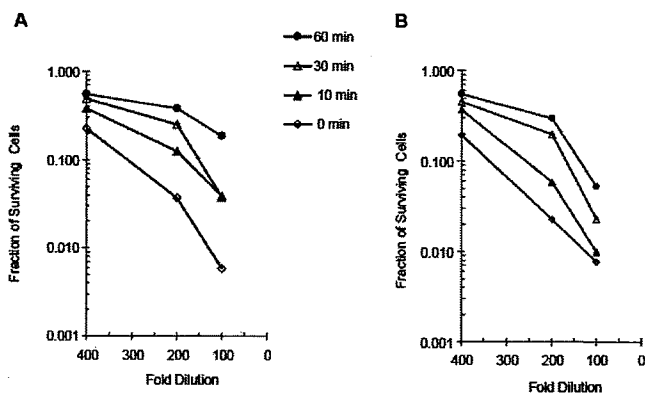

[Figure excerpted from Sponsor]

Appears This Way
On Original

Aliquots of the incubation mixtures were withdrawn at each time point and incubated with HCT116 human colon carcinoma cells at different dilutions (100, 200, and 400-folds). Cytotoxicity was assessed by the clonogenic cell survival assay. In two repeated studies (BMSR-2433 and BMSR-2506), it was shown that cytotoxicity of the microsomal mixtures decreased with increasing incubation time (Figure 2A and 2B).

Figure 2:   Cytotoxicity of ixabepilone-containing microsomal mixtures at
                 various times of incubation. (A) Study No. BMSR-2433 and
                 (B) Study No. BMSR-2506

Ixabepilone (10 µM) was incubated with human liver microsomal preparations at 37°C. At various times
(0, 10, 30 and 60 minutes) following the initiation of incubation, aliquots of the incubation mixtures were
withdrawn and treated with ethanol to terminate the reaction. The concentration of ixabepilone related
compounds in the ethanolic solution was 5 µM. The ethanol extracts were used to treat HCT116 human
colon carcinoma cells at various diluted strength (100, 200 and 400-folds).

[Figure excerpted from Sponsor]

As shown in Table 1, without preincubation (0 min), the microsomal mixtures were highly cytotoxic killing 96.3% (surviving fraction = 0.037) and 97.7% (surviving fraction = 0.023) of the cancer cells in Study No. BMSR-2433 and BMSR-2506, respectively. Table 1 also shows that as the incubation time increased, the fraction of cancer cells surviving treatment increased proportionally.

Table 1:   The cytotoxicity of ixabepilone metabolite mixtures formed from
                incubation with human liver microsomes at various times following
                co-incubation correlates with the amount of ixabepilone remaining in
                the microsomal mixtures

Experiment No.	Incubation Time (min)	% of ixabepilone remaining (by LC/MS/MS)	Cytotoxicity (surviving fraction)[a]	% of ixabepilone equivalent remaining estimated by cytotoxicity
BMSR-2433	0	100	0.037	100
	10	66	0.124	59
	30	41	0.250	43
	60	26	0.382	26
BMSR-2506	0	100	0.023	100
	10	65	0.058	81
	30	46	0.195	50
	60	31	0.296	43

[a] Fraction of HCT116 cells surviving treatment.

[Table excerpted from Sponsor]

Figure 3A and 3B shows the calibration curves of ixabepilone cytotoxicity (conducted in parallel with the microsomal experiments). The calibration curves shows that the percentage of ixabepilone remaining in the incubation mixtures based on the cytotoxicity assay was similar to that determined by HPLC/MS/MS (Table 1). Therefore, the study suggests that the mixture of oxidative metabolites formed from the hepatic metabolism of ixabepilone does not appear to contribute to the overall cytotoxicity of ixabepilone therapy.

Figure 3:   Cytotoxicity of ixabepilone at various concentrations against the HCT116 human colon carcinoma cell line. (A) Study No. BMSR-2433 and (B) Study No. BMSR-2506
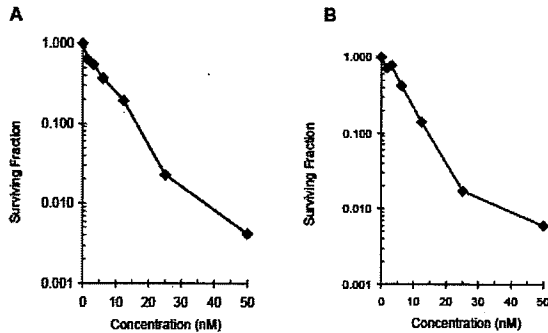
[Figure excerpted from Sponsor]

2.6.4.6 Excretion

930009767: Tissue Distribution and Excretion of Total Radioactivity Following Intravenous Administration of [^{14}C] BMS-247550 to Male and Female Long-Evans Rats – Mass Balance Report

The excretion of radioactivity of [^{14}C] BMS-247550 was examined following a single intravenous dose of 2.75 mg/kg to male and female rats. Urine and feces were collected from 0-8, 8-24, and at 24-hour intervals through 168 hours postdose. Urine, feces, cage rinse, cage wash, cage wipe, and residual tissues and carcasses were analyzed for total radioactivity. Feces was the primary route of elimination of radioactivity. Table 1 shows that at 168 hours postdose, feces and urine accounted for mean values of 81.9 and 11.0% in males and 82.8 and 10.6% in females, respectively. The overall mean recovery of administered radioactivity was 95.8% and 97.1% in males and females, respectively.

Table 1. Mass balance of radioactivity after intravenous administration of [^{14}C] ixabepilone to rats.

Species	Gender	Excretion of Radioactivity % of Dose (Mean ± SD) During 0-168 h			
		Urine	Feces	Others [a]	Total
Rat	Male	11.0 ± 0.9	81.9 ± 0.6	2.96	95.8 ± 1.3
	Female	10.6 ± 0.9	82.8 ± 1.2	3.69	97.1 ± 2.1

SD= standard deviation
NA = not applicable

[Table excerpted from Sponsor]

ι ──────── '930009760: Absorption, Metabolism, and Excretion of Total Radioactivity Following Intravenous Administration of $[^{14}C]$ BMS-247550 to Dogs

The absorption, metabolism, and excretion of, radioactivity of $[^{14}C]$ BMS-247550 was assessed following a single intravenous dose of 0.5 mg/kg to male and female dogs. Blood, plasma, urine, and feces were analyzed for total radioactivity. Selected urine, feces, and plasma samples were examined for metabolite profiles and structure characterization.

Tables 2 and 3 shows mean plasma Cmax levels in males and females were 88.1 and 131 ng equivalents $[^{14}C]$ BMS-247550/g, respectively. Mean concentrations of radioactivity decreased slowly and at 24 hours were 27.8 and 29.4 ng equivalents $[^{14}C]$ BMS-247550/g, respectively, in males and females. Feces was the primary route of elimination for radioactivity. Table 4 shows that radioactivity was slowly eliminated and by 168 hours post-dose, urine and feces accounted for mean values of 5.36 and 80.2%, respectively, in males and 6.95 and 78.1%, respectively, in females. The overall mean recovery of dosed radioactivity was 89.1 and 89.2% in males and females, respectively.

Table 2
Concentrations of radioactivity in blood and plasma at specified times after an intravenous administration of $[^{14}C]$BMS-247550 (0.5 mg/kg) to male purebred beagle dogs

Collection	ng Equivalents $[^{14}C]$BMS-247550/g				
Time	Animal Number				
(Hours)	H06473	H06475	H06476	Mean	SD
Blood					
0.5				84.6	14.2
1				68.1	5.8
4				43.9	4.7
8				35.6	4.6
12				30.4	4.9
24				25.6	2.9
Plasma					
0.5				88.1	19.8
1				75.0	9.8
4				44.5	6.0
8				33.4	6.0
12				32.5	4.6
24				27.8	2.9

SD   Standard deviation.

Appears This Way
On Original

Table 3
Concentrations of radioactivity in blood and plasma at specified times after an intravenous administration of [^{14}C]BMS-247550 (0.5 mg/kg) to female purebred beagle dogs

Collection Time (Hours)	ng Equivalents [^{14}C]BMS-247550/g				
	Animal Number				
	H06477	H06478	H06480	Mean	SD
Blood					
0.5				108	10
1				85.8	6.3
4				50.7	8.4
8				32.2	NA
12				31.0	7.4
24				23.1	5.9
Plasma					
0.5				131	23
1				98.8	17.9
4				54.1	14.6
8				38.4	15.3
12				34.4	11.3
24				29.4	9.1

NA   Not applicable.
NS   No sample. Laboratory accident.
SD   Standard deviation.

a   Single aliquot.

[Tables excerpted from Sponsor]

Appears This Way
On Original

Table 4. Mass balance of radioactivity after intravenous administration of [^{14}C] ixabepilone to dogs.

Species	Gender	Excretion of radioactivity % of dose (Mean ± SD) during 0-168 hours			
		Urine	Feces	Others	Total
Dog	Male	5.36 ±0.62	80.2 ±3.5	3.55	89.1 ±1.2
	Female	6.95 ±2.27	78.1 ±5.4	4.07	89.2 ±1.5

930012038: Biotransformation of [^{14}C] ixabepilone after Intravenous Administration to Bile Duct Cannulated (BDC) Rats

The biotransformation and identification of major metabolites of [^{14}C]ixabepilone in bile duct cannulated rats was determined. Two groups of rats (2/sex/dose) were given a single intravenous dose of [^{14}C] ixabepilone. at 5 mg/kg. Plasma was collected at 2, 8, 12 and 24 hour intervals. Bile and urine was collected at 0-12 and 12-24 hour intervals. Samples were analyzed by HPLC and LS/MS.

Results are as follows:

− In rats, biliary excretion is the major excretion route for [^{14}C] ixabepilone.
− Within 24 hours after dosing, approximately 53% and 15% of the dose was excreted in bile and urine, respectively.
− A small amount of the parent compound (approximately 1% and 2% of the dose in bile and urine, respectively) was excreted unchanged.
− Ixabepilone is the major radioactive component in plasma and is measurable up to 24 hours after dosing.   known degradants, BMS-249798, BMS-326412   were also detected in plasma.
− The major metabolic pathway in rats is oxidation resulting in the formation of the following metabolites: M+32, M+30, M+28, M+16, M+14, M+12, M-4 and M-2. Twenty-six metabolites were identified in bile and six in urine. No metabolite was characterized.
− The major drug-related compounds identified in urine are ixabepilone, M8, M34 and M41.

930012773: Metabolism of [^{14}C] ixabepilone (BMS-247550) Following Intravenous Administration to Male and Female Rats and Dogs

The biotransformation profiles in plasma, urine and feces and the extent of the elimination of [^{14}C] ixabepilone was determined in male and female rats and dogs. Rats and dogs were administered 2.75 and 0.5 mg/kg dose of [^{14}C] ixabepilone via intravenous infusion. Plasma (at 1, 4, 8 and 24 hours), urine and feces (both at 0-168 hours) samples were collected and biotransformation profiling of radioactivity was performed to determine the percent distribution. Samples were analyzed by LC/MS to identify metabolites of ixabepilone.

66

Results are summarized below:

- In rats and dogs, feces was the primary route of elimination accounting for >80% of the dose during the collection period (0-168 hours). Urine contained ≤11% of the dose in rats (both males and females) and dogs following IV administration.
- [^{14}C]Ixabepilone is extensively metabolized in rats and dogs. A total of 16 metabolites and 4 degradants were identified in both species. Metabolites identified in urine and feces included mono- and di-oxygenated metabolites (M+34, M+28, M+16, M+14 and M+12 metabolites) and M-2 and M-4 metabolites.
- In rat and dog plasma, ixabepilone is the major component detected during the 24 hour period. In both species, two major degradants, BMS-249798 and BMS-326412, were identified in the plasma. The parent drug, [^{14}C] ixabepilone, is the major component identified in both rat and dog urine.

Species/Strain	Rat/Sprague Dawley, bile-duct cannulated
Gender (M/F)/Number of animals:	M/2 per treatment/sample time or time period
Feeding condition:	Not specified
Vehicle/Formulation:	1:1:3:5 Cremophor EL/ethanol/phosphate buffer/PEG300
Method of Administration:	Single dose IV
Dose:	Study NAPR 2187: 5 mg/kg (14.8 μCi/kg); Study 2297: 3.8 mg/kg (10.3 μCi/kg) [a]
Radionuclide:	^{14}C
Specific Activity:	2.7 μCi/mg

Ixabepilone and Metabolites	% Distribution of Radioactivity [b]					
	Bile (% of Dose)	Urine (% of Dose)	Plasma (% of Sample)			
	(0-24 h)	(0-24 h)	2 h	8 h	12 h	24 h
Ixabepilone	0.96	2.13	42.7	84.6	62.5	58.6
BMS-249798 [c]	1.38	0.42	4.8	15.4	37.5	8.0
_____ [?]	1.23	0.33	ND [d]	ND	ND	5.7
M2, M21	1.23	ND	ND	ND	ND	ND
M18, M34, M35, BMS-326412 [e]	2.97 [?]	1.61 [f]	15.2 [g]	ND	ND	27.6 [g]
M9	1.06	0.27	ND	ND	ND	ND
M19	0.80	ND	ND	ND	ND	ND
M22	0.80	ND	ND	ND	ND	ND

Ixabepilone and Metabolites	% Distribution of Radioactivity [b]					
	Bile (% of Dose)	Urine (% of Dose)	Plasma (% of Sample)			
	(0-24 h)	(0-24 h)	2 h	8 h	12 h	24 h
M23	0.85	ND	ND	ND	ND	ND
M24	1.86	ND	ND	ND	ND	ND
M25	0.64	ND	ND	ND	ND	ND
M26	1.01	ND	ND	ND	ND	ND
M27	1.01	ND	ND	ND	ND	ND
M28	1.81	ND	ND	ND	ND	ND
M29	1.81	ND	ND	ND	ND	ND
M30, M31	1.59	ND	ND	ND	ND	ND
M32, M33	2.34	ND	ND	ND	ND	ND
M36	1.06	ND	ND	ND	ND	ND
M37, M38	1.70	ND	ND	ND	ND	ND
M39	1.01	ND	ND	ND	ND	ND
M40	1.11	ND	ND	ND	ND	ND
M41	ND [e]	0.93	5.1	ND	ND	ND
Others [h]	24.90	9.24	32.4	ND	ND	ND
Total	53.11	14.95	100.2	100.0	100.0	99.9

Additional Information: 1) Samples from all animals (n=2) at a particular timepoint or time interval were pooled. The metabolites were identified by LC/MS analysis. Structures of degradants, BMS-249798, BMS-326412 and _____ in samples were confirmed by comparison of their HPLC retention times and MS fragmentations to those of synthetic standards. 2) An exploratory study with BDC rats was conducted with non-radiolabeled ixabepilone to identify metabolites of ixabepilone (910074578). The results from study are not presented as a tabulated summary because quantification of metabolite distribution could not be made.

[a] The urine and bile samples used for the analyses were obtained from study NAPR 2187. Two extra rats were dosed in study NAPR 2297 to obtain an additional 24-h plasma sample for the HPLC profiling and LC/MS identification.

[b] The relative distribution of ixabepilone and its metabolites in bile and urine is expressed as the % of the dose that each radioactive component represents in a particular matrix. The relative distribution in plasma is expressed as the % distribution of radioactivity of each radioactive component in the sample extract.

[Table excerpted from Sponsor]

Best Possible Copy
Appears This Way
On Original

2.6.4.7 Pharmacokinetic drug interactions

Xt043022/930012012: *In Vitro* Evaluation of Ixabepilone (BMS-247550) as an Inducer of Cytochrome P450 Expression in Cultured Human Hepatocytes

The potential of ixabepilone to induce cytochrome P450 enzymes (CYP1A2, CYP2B6, CYP2C9 and CYP3A4/5) was investigated using primary cultures of human hepatocytes *in vitro*. Cultured human hepatocytes was treated with ixabepilone at different concentrations (0.06, 0.6, 6 and 20 µM) and known CYP inducers. Incubations with known CYP enzymes were conducted with microsomes to evaluate enzyme activity. In addition, cell lysates were prepared from hepatocytes and levels of mRNA encoding CYP enzymes was measured using branched DNA analysis. Treatment of cultured human hepatocytes with 20 µM of BMS-247550 did not cause a statistically significant increase in the activities of CYP1A2, CYP2B6, CYP2C9 or CYP3A4/5. In addition, treatment of cultured human hepatocytes with ixabepilone had no effect on mRNA levels of CYP1A2, CYP2B6, CYP2C9 or CYP3A4. The CYP inducers (omeprazole, phenobarbital and rifampin) caused increases in CYP activity and mRNA levels. Results of the LDH analysis indicate that treatment of cultured human hepatocytes with ixabepilone did not result in cytoxicity. The study suggest ixabepilone at concentrations up to 20 µM does not appear to be an inducer of CYP1A2, CYP2B6, CYP2C9 or CYP3A4/5 and does not show to cause drug-drug interactions with co-administered drugs that are metabolized by these CYP enzymes *in vivo*. Results are summarized in the table below.

Test Article	Concentration (µM)	CYP Enzyme Activity - Fold Change as Compared to 0.1% DMSO Control[a]			
		CYP1A2	CYP2B6	CYP2C9	CYP3A4/5
DMSO control	0.1%	1.00±0.07[b]	1.00±0.62[b]	1.00±0.18[b]	1.00±0.49[b]
Ixabepilone	0.06 µM	1.14±0.26	1.09±0.21	1.13±0.23	1.28±0.40
Ixabepilone	0.6 µM	1.10±0.14	0.842±0.079	0.908±0.117	1.00±0.29
Ixabepilone	6 µM	1.22±0.21	1.24±0.26	1.16±0.17	1.76±0.91
Ixabepilone	20 µM	1.27±0.23	1.32±0.37	1.28±0.27	2.36±1.51
Omeprazole[c]	100 µM	15.0±4.1	7.67±4.78	1.44±0.41	3.12±1.74
Phenobarbital[c]	750 µM	2.52±0.29	13.0±5.5	1.96±0.61	8.06±4.17

Test Article	Concentration (µM)	CYP Enzyme Activity - Fold Change as Compared to 0.1% DMSO Control[a]			
		CYP1A2	CYP2B6	CYP2C9	CYP3A4/5
Rifampin[c]	10 µM	2.25±0.21	5.64±1.12	2.33±0.69	8.69±4.29
		mRNA Levels of CYP Enzymes - Fold Change[a]			
Test Article	Concentration	CYP1A2	CYP2B6	CYP2C9	CYP3A4
DMSO control	0.1%	1.00±0.45	1.00±0.23	1.00±0.60	1.00±0.61
Ixabepilone	0.06 µM	1.42±0.18	1.19±0.85	0.686±0.253	0.764±0.404
Ixabepilone	0.6 µM	1.46±0.21	1.08±0.34	1.22±0.38	1.14±0.39
Ixabepilone	6 µM	1.86±0.38	1.54±0.70	1.26±0.85	1.91±1.07
Ixabepilone	20 µM	1.66±0.54	1.49±0.65	1.95±0.50	3.39±3.02
Omeprazole[c]	100 µM	218±102	NA	NA	NA
Phenobarbital[c]	750 µM	NA	8.01±1.91	NA	NA
Rifampicin[c]	10 µM	NA	5.65±2.84	2.75±2.14	10.1±6.5

Additional Information: These results suggest that ixabepilone is not likely to be an inducer of CYP1A2, 2B6, 2C9 or 3A4 at concentrations ≤20 µM.

[a] Microsomal activity rates and mRNA levels for each of the CYP enzymes were determined separately for each individual donor. Fold-change for each enzyme for each donor was then calculated and is presented as fraction or as fold increase over control (control incubations with 0.1% DMSO). Values are the mean ± standard deviation of three human hepatocyte preparations.

[b] Values represent the mean ± CV.

[c] Positive control reference compounds.

NA = Not applicable, CYP mRNA not measured for treatment group.

[Table excerpted from Sponsor]

Xt045016/930012272: *In Vitro* Evaluation of Ixabepilone (BMS-247550) as an Inhibitor of Human Cytochrome P450 Enzymes

The potential of ixabepilone to inhibit cytochrome P450 enzymes was investigated *in vitro* using human liver microsomes. To evaluate ixabepilone as a direct inhibitor of CYP activity, human liver microsomes were incubated with probe substrates and NADPH in the presence of different concentrations of ixabepilone (0.05 to 30 µM). Probe substrates are indicated in Table 5. In addition, to investigate the potential of ixabepilone to function as a metabolism-dependent inhibitor (at the same concentration), ixabeopilone was pre-incubated with human liver microsomes in the presence of NADPH generating system for 30 minutes before incubation with probe substrates. Specific products of the CYP reaction with the probe substrate were quantified by LC/MS analysis.

Ixabepilone showed direct inhibition of CYP3A4/5 with an $IC_{50} = 15$ µM. Ixabepilone did not directly inhibit CYP1A2, CYP2A6, CYP2B6, CYP2C8, CYP2C9, CYP2C19, CYP2E1, or CYP2D6, with IC_{50} values greater than the highest concentration of ixabepilone given (30 µM). Ixabepilone was a metabolism-dependent inhibitor of CYP3A4/5 with an increase in inhibition observed with $IC_{50} = 9$ and 3 µM for testosterone 6β-hydroxylation and midazolam 1'-hydroxylation, respectively. For all the other enzymes studied ixabepilone caused little to no metabolism-dependent inhibition, as there was no increase in inhibition upon pre-incubation. Data are summarized below in Sponsor's Table 5.

The metabolism-dependent parameters (K_I and K_{inact}) for the inhibition of CYP3A/5 by ixabepilone are presented in Table 6. The calculated K_I value for the inactivation of CYP3A4/5 by ixabepilone upon pre-incubation with an NADPH-generating system was 7.5 µM. Ixabepilone inactivated CYP3A4/5 as measured by midazolam 1'-hydroxylation . with a K_{inact} value of 0.043 min-1.

Appears This Way
On Original

Table 5:   Summary of results: *In vitro* evaluation of BMS-247550 as an inhibitor of human CYP enzymes

Enzyme	CYP reaction	Zero-minute pre-incubation		30-minute pre-incubation		Potential for metabolism-dependent inhibition[b]
		IC50 (µM)	Maximum inhibition at 30 µM (%)[a]	IC50 (µM)	Maximum inhibition at 30 µM (%)[a]	
CYP1A2	Phenacetin *O*-deethylation	> 30	NA	> 30	NA	little or no
CYP2A6	Coumarin 7-hydroxylation	> 30	14	> 30	NA	little or no
CYP2B6	Bupropion hydroxylation	> 30	3.8	> 30	19	little or no
CYP2C8	Paclitaxel 6α-hydroxylation	> 30	8.3	> 30	11	little or no
CYP2C9	Diclofenac 4'-hydroxylation	> 30	18	> 30	17	little or no
CYP2C19	*S*-Mephenytoin 4'-hydroxylation	> 30	17	> 30	7.6	little or no
CYP2D6	Dextromethorphan *O*-demethylation	> 30	6.7	> 30	0.90	little or no
CYP2E1	Chlorzoxazone 6-hydroxylation	> 30	NA	> 30	NA	little or no
CYP3A4/5	Testosterone 6β-hydroxylation	> 30	12	9.0 ± 0.6	73	yes
CYP3A4/5	Midazolam 1'-hydroxylation	15 ± 1	66	3.0 ± 0.2	91	yes

Notes   Values were calculated using the average data obtained from duplicates for each incubation condition. The IC50 values were calculated using XLFit.

a   Maximum inhibition (%) is calculated using the following formula and data for the highest concentration of BMS-247550 for which usable data were collected (results are rounded to two significant figures): Maximum inhibition (%) = 100% – Percent of solvent control activity (see **Appendix 8**)

b   Metabolism-dependent inhibition was determined by comparison of IC50 values with and without pre-incubation and by visual inspection of IC50 plots.

NA   Inhibition was not observed at the highest concentration of BMS-247550 studied (30 µM) as indicated by a "percent of solvent control activity" greater than 100%.

Table 6.

Inhibitor Tested	K_i and k_{inact} Values CYP3A4 (Midazolam 1'-hydroxylation)	
	K_i (µM)	k_{inact} (min⁻¹)
Ixabepilone	7.5	0.043
Troleandomycin[a]	0.53	0.18

Additional Information: These results suggest that ixabepilone is a weak metabolism-dependent inhibitor of CYP3A4/5 compared to troleandomycin.

a   Positive control incubation was performed using known metabolism-dependent inhibitor of CYP3A4: troleandomycin.

[Tables excerpted from Sponsor]

Appears This Way
On Original

920007704: A study to assess the potential for inhibition of human cytochrome P450 by BMS-247550.

The inhibitory activity of BMS-247550 on human cytochrome P450 was assessed. To measure the inhibitory activity of BMS-247550, IC_{50} values for BMS-247550 activity was determined using CYP1A2, CYP2C9, CYP2C19 and CYP2D6 or CYP3A4 as substrates. BMS-247550 did inhibit CYP3A4 with an IC50 value of 7.3 μM (weak inhibitor). BMS-247550 did not inhibit CYP1A2, CYP2C9, CYP2C19 and CYP2D6 at the highest concentration tested (IC_{50}>200 μM). Data suggests that BMS-247550 appears to have minimal potential to alter the metabolic clearance of drugs that are highly metabolized by CYP3A4 and unlikely to significantly alter metabolic clearance of drugs metabolized by CYP1A2, CYP2C9, CYP2C19 and CYP2D6. The table below shows IC_{50} values for the inhibition of CYP isoforms.

IC_{50} Values (μM; mean of two determinations)

Test Substance	CYP1A2	CYP2C9	CYP2C19	CYP2D6	CYP3A4
BMS-247550	>200	>200	>200	>200	7.3

[Table excerpted from Sponsor]

930012647: Identification of Enzymes Involved in the Metabolism of Ixabepilone (BMS-247550)

The *in vitro* metabolism of ixabepilone was investigated by incubating the compound with human cDNA-expressed CYP enzymes and to evaluate the inhibition effects of chemical inhibitors on the biotransformation of ixabepilone was investigated. Ixabepilone (BMS-247550) was incubated with human CYP enzymes (CYP1A2, CYP2B6, CYP2D6, CYP2E1, CYP3A4, CYP3A5, CYP2C8, CYP2C9 and CYP2C19). Samples were analyzed by LC/MS. Study showed that ixabepilone was mainly metabolized by CYP3A4 and CYP3A5 with the formation of several M+16 metabolites (M2, M3, M8, M9, M10, M11) and two M-2 metabolites (M19 and M20). CYP3A4 also formed several M+14 metabolites (M4, M5, M14, M15, M16 and M17). These metabolites were also detected in incubations with the liver microsomes of mouse, rat, dog, monkey, and human. CYP2D6 and CYP2C19 also metabolized ixabepilone, forming M9, a minor metabolite. To evaluate the inhibition effects of the chemical inhibitors on the oxidative metabolism of ixabepilone, the drug was incubated in human liver microsomes in the presence of CYP inhibitors (ketoconazole for CYP3A4, troleandomycin for CYP3A4, montelukast for CYP2C8 and 1-aminobenzotriazole for all CYP enzymes). Incubation of ixabepilone in human liver microsomes in the presence of CYP inhibitors confirmed that CYP3A4 was the major CYP enzyme involved in the *in vitro* oxidative metabolism of ixabepilone. In conclusion, CYP3A4 and CYP3A5 were the major human CYP enzymes that were responsible for the oxidation metabolism of

ixabepilone. CYP2D6 and CYP2C19 were also involved in the oxidative metabolism of ixabepilone. Results are summarized in the Sponsor's table below.

Formation of Metabolites [a]	Incubation system - cDNA-Expressed CYP Enzymes			
	CYP3A4	CYP3A5	CYP2D6	CYP2C19
Ixabepilone	+	+	+	+
BMS-249798	+	+	+	+
BMS-326412	+	+	+	+
M2	+	-	-	-
M3	+	-	-	-
M4	+	-	-	-
M5	+	-	-	-
M8	+	+	-	-
M9	+	+	+	+
M10	+	+	-	-
M11	+	+	-	-
M14	+	-	-	-
M15	+	-	-	-

Formation of Metabolites [a]	Incubation system - cDNA-Expressed CYP Enzymes			
	CYP3A4	CYP3A5	CYP2D6	CYP2C19
M16, M17	+	-	-	-
M19	+	+	-	-
M20	+	+	-	-

Additional Information: Incubations with CYP1A2, CYP2B6, CYP2E1, CYP3A4, CYP3A5, CYP2C8 and CYP2C9 were also conducted, but no metabolites were detected in these incubations.

[a] Since the incubations were performed with unlabeled ixabepilone, the exact integration of the peaks were not available. The "+" and "-" signs are to indicate that the metabolites are "detected" or "not detected" by LC/MS, respectively.

[Table excerpted from Sponsor]

930018090: Identification of Enzymes Involved in the Metabolism of Ixabepilone (BMS-247550), Study 2

In this study, the effects of chemical and antibody inhibitors of CYP enzymes on ixabepilone metabolism in human liver microsomes (HLM) was evaluated and the metabolism kinetics of ixabepilone in HLM and expressed CYP3A4 was determined. The study also confirmed the CYP enzymes responsible for the metabolism of ixabepilone by incubation with human cDNA expressed enzymes (as shown previously in Study No. 930012647). To identify the enzymes responsible for its metabolism, ixabepilone at 0.5 µM was incubated with human liver microsomes in the presence of selective chemical CYP inhibitors and in the presence of monoclonal antibodies that are inhibitory to human CYPs. Ixabepilone at 0.5 µM was also incubated with human cDNA-expressed enzymes (CYP1A2, 2A6, 2C8, 2C9, 2C19, 2D6, 3A4). As shown in

Appears This Way
On Original

72

the   table   below,   ixabepilone   was   metabolized   by   CYP3A4.

Table 10:   Oxidative Metabolism of Ixabepilone in Human Liver
                         Microsomes in the Presence of CYP Inhibitors (n = 3)

Treatment/ Inhibitor	Enzyme Inhibited	Ixabepilone Remaining		Ixabepilone Metabolized (%)	% Inhibition[c]
		nM[a]	%[b]		
Positive Control	-	88.6	35.5	64.5	-
Heat Killed	-	249.5	100[d]	0	-
No NADPH	-	268	100[d]	0	-
Furafylline	CYP1A2	117.4	47.1	52.9	17.9
Tranylcypromine	CYP2A6	111.9	44.9	55.1	14.5
Montelukast	CYP2C8	135.6	54.4	45.6	29.2
Sulfaphenazole	CYP2C9	110.1	44.1	55.9	13.4
Benzylnirvanol	CYP2C19	96.3	38.6	61.4	4.8
Quinidine	CYP2D6	100.7	40.4	59.6	7.5
Ketoconazole	CYP3A4	234	93.8	6.2	90.4

[a] Average of triplicates.

[b] % Remaining was calculated as follows: nmole of ixabepilone in the incubation mixture with inhibitor / nmole of ixabepilone in the negative control (heat killed) x 100 (nmoles were determined from LC/MS analysis).

[c] % Inhibition = (% ixabepilone remaining – % ixabepilone in positive control) / (% ixabepilone in negative control – % ixabepilone in positive control).

d The amount of ixabepilone in the negative control samples was designated as 100% as the peak area ratio of the parent drug to IS in the incubations was designated as 100%.

Table 11:   Oxidative Metabolism of Ixabepilone in Human Liver
                         Microsomes in the Presence of Monoclonal Antibodies (n = 3)

Treatment	Ixabepilone Remaining		Ixabepilone Metabolized (%)	% Inhibition[c]
	nM[a]	%[b]		
Positive Control	110.7	47.2	52.8	-
No NADPH	234.7	100[d]	0	-
Control - With Antibody Against Hen Egg White[e]	93.8	40.0	60.0	NI[f]
With Anti-CYP3A4	213.1	90.8	9.2	82.6
With Anti-CYP1A2	87.1	37.1	62.9	NI[f]
With Anti-CYP2C8	96.0	40.9	59.1	NI[f]
With Anti-CYP2C9	93.6	39.9	60.1	NI[f]
With Anti-CYP2C19	88.0	37.5	62.5	NI[f]
With Anti-CYP2D6	99.0	42.2	57.8	NI[f]

[a] Average of triplicates.

[b] % Remaining was calculated as follows: nmole of ixabepilone in the incubation mixture with inhibitor / nmole of ixabepilone in the negative control (heat killed) x 100 (nmoles were determined from LC/MS analysis).

[c] % Inhibition = (% ixabepilone remaining – % ixabepilone in positive control) / (% ixabepilone in negative control – % ixabepilone in positive control)

[d] The amount of ixabepilone in the negative control samples was designated as 100% as the peak area ratio of the parent drug to IS in the incubations was designated as 100%.

[e] Control incubation contained a monoclonal antibody against hen egg white lysozyme to assess for nonspecific reactions.

[f] NI: No Inhibition; % of ixabepilone remaining was ≤ % of ixabepilone in the positive control incubation sample.

[Tables excerpted from Sponsor]

To determine Km and V_{max} values for its metabolism, ixabepilone was incubated with HLM at concentrations ranging from 0.1 to 25 µM and CYP3A4 at concentrations ranging from 0.1 to 100 µM. The table below shows the Km values for the oxidative metabolism of ixabepilone were 8.19 µM in HLM and 4.26 µM in CYP3A4. The V_{max} values were 1399.03 nmole/mg protein/min and 17.87 nmole/pmole CYP/min in HLM and CYP3A4. Therefore, at clinically relevant concentrations, ixabepilone is oxidized by CYP3A4 *in vitro*.

(D) Determination of kinetic parameters for the oxidative metabolism of ixabepilone in HLM and CYP3A4 [d]		
Study System	Km (µM)	Vmax
HLM	8.19	1399 nmole/mg protein/min
CYP3A4	4.26	17900 nmole/nmole CYP/min
Additional information: CYP3A4 is responsible for the oxidative metabolism of ixabepilone.		

[a] % Inhibition = (% ixabepilone remaining − % ixabepilone in positive control) / (% ixabepilone in negative control − % ixabepilone in positive control).
[b] The amount of ixabepilone in the negative control samples was designated as 100%.
[c] % of ixabepilone in buffer control was assumed to be 100%.
[d] Kinetic values were estimated from nonlinear regression assuming Michaelis-Menten kinetics V = Vmax * S/(Km +S), where S is ixabepilone concentration. conc.: concentration; CYP: cytochrome P450; HLM: human liver microsomes; LLOQ: lower limit of quantitation; NA: Not Applicable; NI: No Inhibition

[Table excerpted from Sponsor]

2.6.4.8 Other Pharmacokinetic Studies – None

2.6.4.9 Discussion and Conclusions

Ixabepilone had a long elimination half-life. The terminal half-life ($T_{½}$) in mice (IV administration) and rat (intra-arterial administration) ranged from approximately 3 to 9.6 hours to 24 hours in dogs (IV administration). Clinically, mean $T_{½}$ was approximately 35 hours after 3-hour IV infusion of 40 mg/m². The longer half-life in dogs and humans compared to mice and rats may be attributed to the longer blood sampling scheme. Ixabepilone showed moderate to high clearance in mouse, rat and dog. The systemic clearances were 68, 56, and 17 mL/min/kg in mouse, rat, and dog, respectively. Ixabepilone also had a high mean steady-state volume of distribution (6.3, 23, and 25 L/kg in mouse, rat, and dog, respectively).

Ixabepilone is extensively bound in mouse serum proteins (92.4% at 5000 ng/mL) and is moderately bound in rat, dog and human serum proteins (44 to 67%). The extent of serum-protein binding decreased in rat, dog, and human with increasing concentration over the concentration range of 50 to 5000 ng/mL. Ixabepilone showed moderate distribution into blood cells except high distribution at the nominal concentration of 50 ng/mL in rat and dog.

Drug-related radioactivity was extensively distributed in the tissues in male and female rats after IV administration of radiolabeled ixabepilone. There were no apparent gender-related differences in the distribution of ixabepilone derived radioactivity in blood, plasma, and tissues. The highest percentages of administered radioactivity were associated with liver, muscle, nonpigmented skin, and pigmented skin. Low levels of radiolabeled ixabepilone-derived radioactivity were detected in the cerebellum, spinal cord, and testes, suggesting that the drug-derived radioactivity crossed the blood/brain and blood/testes barriers. Ixabepilone-derived radioactivity was distributed in maternal and fetal tissues and excreted in milk. The milk: plasma concentration ratios ranged from 0.296 to 2.64.

Metabolites of ixabepilone identified in rats, dogs, and humans were all products of oxidative biotransformation and included M+34, M+32, M+30, M+28, M+18, M+16, M+14, M+12, M-2, and M-4 metabolites. Metabolites identified in rat and dog plasma, urine or feces were also detected in incubations with liver microsomes from mouse, rat, dog, monkey, and human. The known degradants of ixabepilone, BMS-249798, BMS-326412 ⸻⸻ were also detected in the plasma, urine, and feces of rats and dogs. The degradants accounted for less than 10% of the administered dose. The metabolite and degradant profile in rat and dog plasma was similar with unchanged ixabepilone being the most abundant drug-related component.

The major human CYP enzymes that were responsible for the *in vitro* oxidative metabolism of ixabepilone were CYP3A4/5. Ixabepilone did not inhibit the activities of CYP enzymes 1A2, 2A6, 2B6, 2C8, 2C9, 2C19, 2D6, and 2E1 in human liver microsomes. The drug did inhibit CYP3A4 in a metabolism dependent manner. However, based on the plasma concentration of ixabepilone in cancer patients and the in vitro parameters (K_I and k_{inact}), ixabepilone should have a low potential for inhibition of CYP3A4/5.

Fecal excretion played a major role in the elimination of ixabepilone in rats and dogs. Following an IV dose, ixabepilone-derived radioactivity was excreted primarily in the feces (> 64%) in rats, and dogs, of the dose was excreted in the urine of each species. Following an IV dose of radioactive ixabepilone to bile duct-cannulated rats, approximately 53% of the radioactivity was excreted in the bile and about 15% was excreted in the urine. In intact rats and dogs, a small fraction of the radioactivity in feces ($\leq$ 2.1%) and urine (< 3%) was attributed to the parent compound. These results indicated that metabolism played a major role in the elimination of the drug in rats and dogs.

Systemic exposure after intermittent dosing was approximately dose proportional in 6-month rat and 9-month dog toxicology studies. No gender-related difference in exposure of ixabepilone was observed in the dog study. In the rat study, however, Cmax values from males at the HD (6.7 mg/kg or 40.2 mg/m^2) were 3-fold higher compared to females.

Appears This Way
On Original